

# CLASSIFICATION OF LAND COVER USING MODEL BASED DECOMPOSITION TECHNIQUES FOR PALSAR DATA

## A DISSERTATION

*Submitted in partial fulfillment of the  
requirements for the award of the degree*

*of*

**MASTER OF TECHNOLOGY**

*in*

**ELECTRONICS AND COMMUNICATION ENGINEERING**

**(With Specialization in RF & Microwave Engineering)**

By

**ASHIS KUMAR BEHERA**



**DEPARTMENT OF ELECTRONICS AND COMMUNICATION ENGINEERING  
INDIAN INSTITUTE OF TECHNOLOGY ROORKEE  
ROORKEE - 247 667 (INDIA)**

**JUNE, 2014**

## CANDIDATE'S DECLARATION

---

---

I hereby declare that the work, presented in this dissertation report, entitled “**CLASSIFICATION OF LAND COVER USING MODEL BASED DECOMPOSITION TECHNIQUES FOR PALSAR DATA**” being submitted in fulfilment of partial requirements for the award of Degree of Master of Technology in RF and Microwave Engineering, Indian Institute of Technology, Roorkee is my original work. The results submitted in this dissertation report have not been submitted for the award of any other Degree or Diploma.

Date:

Place: IIT Roorkee

(Ashis Kumar Behera)

Enrolment # 12533004

ECE Department

IIT Roorkee



---

---

This is to certify that the statement made by the candidate is correct to the best of my knowledge and belief. This is to certify that this dissertation entitled, “**CLASSIFICATION OF LAND COVER USING MODEL BASED DECOMPOSITION TECHNIQUES FOR PALSAR DATA**” is an authentic record of candidate's own work carried out by him under my guidance and supervision. He has not submitted it for the award of any other degree.

Date:

Place: IIT Roorkee

(Prof. Dharmendra Singh)

Professor,

ECE Deptt., IIT Roorkee

## ACKNOWLEDGEMENT

First and foremost, I owe my deepest gratitude to my supervisor, **Prof. Dharmendra Singh**, for his continuous guidance, motivation and support during this research. His vast knowledge, experience and his dedication in imparting this knowledge to the students, makes him a perfect guide. Throughout my thesis-working period, he provided encouragement, sound advice, good teaching and lots of good and motivating ideas. I would have been lost without him. He is an inspiring professor, a great advisor and above all a nice person.

I am also grateful to members of Remote Sensing Lab specially **Miss Pooja Mishra** for introducing me to this interesting field of radar imaging and its applications as well as for the patiently examining whole of my thesis work throughout the year.

I would also like to thank **Mr. Tasneem and Mr. Nazim** for their valuable support and time to time guidance in technical issues, which was instrumental in making this dissertation work a success. Finally, I would also like to thank all my friends, specially **Mr. Amit Singh Bisht and Mr. Sandeep Kumar Shukla** for their support and valuable suggestions.

I am thankful to the Ministry of Human Resource Development (MHRD) for providing financial help. Above all, I thank my parents, my brother and my sister for their love, co-operation and encouragement which was a constant source of inspiration for me.

Last but not least, I thank Almighty God for his blessings and making my work successful.

## ABSTRACT

Microwave Remote sensing data are broadly used in detection and analysis of the land cover and land use features. The purpose of this dissertation is to examine the application of multi-polarized data of ALOS-PALSAR for land cover and land use mapping. For land cover /use classification, the application aspects of information has been analyzed, which are obtained through the fully polarimetric SAR data. There are numerous techniques available in the literature for land cover classification; however uncertainty still persists during the labeling of various clusters to their classes in absence of any other additional information. Henceforth, the theme of our present research work is centered on analyzing the useful intrinsic information taken from SAR observables that are obtained through the various model based decomposition techniques. ALOS PALSAR L-Band fully polarimetric data was used in this study for the entire backscatter analysis. The decomposed outcomes which were retrieved from the aforesaid approach were correlated with the decomposition outcomes from the deorientation method, given by Yamaguchi et.al (2005) utilizing the coherency matrix's rotation, and also from the direct decomposition method without compensating for the shift in orientation angle. As expected beforehand, double bounce scattering from the urban scatters were seen to be enhanced, but the volume scattering component reduced. The response of the several features in the decomposition method using the cosine squared function was analyzed. The relation between the co-polarized and cross-polarized response with the four scattering components was also investigated. The Model Based Decomposition methods (Freeman & Durden 3-component decomposition, original 4-component decomposition, 4-component decomposition with rotation of coherency matrix, new general 4-component decomposition with unitary transformation) have been used to differentiate the classes based on scattering mechanisms. The precision and utility of three supervised classifiers (minimum distance, maximum likelihood, and parallelepiped) have been analyzed for Roorkee region using time-series ALOS-PALSAR data. Here we have compared the different classification methods and their performances or accuracy. The comparison among three classification methods that are maximum likelihood classification, minimum distance and parallelepiped classification have been done. The overall accuracy of these classification methods are critically examined and analyzed. The results obtained from maximum likelihood classifier method, confirm the suitability for the classification of land cover of ALOS PALSAR data very significantly. In coming years this classification method, it would be very essential for

various environmental and socioeconomic applications which comprises the flood mapping, forest and agriculture monitoring.



## Contents

1. Introduction	
1.1. Background Study.....	1
1.2. Introduction to Polarization.....	3
1.3. Scattering, Covariance & Coherency Matrix .....	6
1.4. Motivation of Work .....	8
1.5. Objective of the thesis.....	9
1.6. Dissertation outline .....	9
2. Literature Review	
2.1 Radar Remote Sensing and SAR.....	10
2.2. Use of Remote Sensing For Land Use and Land Cover Change .....	12
2.3. Polarimetric Decompositions.....	14
2.4. Land use classification.....	16
3. Theoretical concept	
3.1 Polarimetric decomposition.....	17
3.2. Model based Decomposition.....	20
3.2.1 Three component scattering model.....	21
3.1.2. The original Four component decomposition	22
3.1.3. Yamaguchi 4-CSPD with rotation of coherency matrix: Y4R	23
3.1.4. New General Four-Component Scattering Power Decomposition with Unitary Transformation of Coherency Matrix	24
3.2. Classification Schemes	27
3.2.1. Parallelepiped classification	20
3.2.1.3. Minimum distance classification	21
3.2.1.3. Maximum likelihood classification	23

<b>4. MATERIAL AND METHODOLOGY</b>	
4.1. Study Area.....	29
4.2. Data Used.....	31
4.3. Software Used.....	32
4.4. Methodology.....	32
4.4.1.Data import.....	34
4.4.2.Multilooking.....	34
4.4.3.coherent matrix generation.....	34
4.4.4.Terrain correction.....	34
4.4.5.Model based decomposition algorithm.....	35
4.5. Classification based on Model based Decomposition.....	39
<b>5. Results and Discussion</b>	
5.1. Model based decomposition .....	39
5.1.1.Three component decomposition	39
5.1.2. Four component decomposition	40
5.1.3. Four component decomposition with rotation of coherency matrix	41
5.1.4. The New Four Component Decomposition Method	43
5.2. Supervised classification .....	45
5.2.1. Supervised classification based on 4- component decomposition	45
5.2.2. Supervised classification based on 4- component decomposition with rotation of coherency matrix	48
5.2.3. Supervised classification based on new general 4-CSPD with unitary Transformation	53
6. Conclusion and Future Work.....	57
References.....	58

## List of figures

2.1.	Polarized and unpolarized of Propagation electromagnetic waves	4
2.3.a.	Surface scattering from a rough surface	19
2.3.b.	Double bounce scattering from a ground and tree trunk	19
2.3.c.	Volume scattering from multiple reflections from the tree branches	19
3.1.	Sketch of three scattering mechanism used in the model	20
3.2.	Sketch of four scattering mechanism used in the model	22
3.3.	Sketch of four scattering mechanism with rotation of theta angle to coherency matrix	24
4.1.	Study area location	30
4.2	Flow chart of methodology	33
4.3.	Flow chart of three component decomposition	35
4.4	Flow chart of four component decomposition	36
4.5	Flow chart of four component decomposition with rotation of coherency matrix	37
4.6	Flow chart of General four component decomposition with unitary transformation of coherency matrix	38
5.1.1.	RGB color coding image three component decomposition	40
5.1.2.	percentage share of different scattering power of three component decomposition	41
5.2.1.	RGB color coding image Four component decomposition	42
5.2.2.	percentage scattering power of Four component decomposition	42
5.3.1	RGB color coding image Four component decomposition with rotation of coherency matrix	43
5.3.2	percentage sharing of scattering power of three component decomposition	44
5.4.1.	RGB color coding image of The New General Component Decomposition	45
5.4.2.	percentage scattering power of The New general decomposition	45



## List of Tables

4.1.	Data set information	30
4.2.	Ground truth survey points for region Roorkee	38
5.2.1.	Pixel assignment of various classes shown by confusion matrix relative to parallelepiped classification	45
5.2.2	User accuracy and producer accuracy (in percent) estimates relative to parallelepiped classification	46
5.2.3.	User accuracy and producer accuracy (in percent) estimates relative to minimum distance classifier	46
5.2.4	Pixel assignment of various classes shown by confusion matrix relative to minimum distance classification	46
5.2.5	User accuracy and producer accuracy (in percent) estimates relative to minimum distance classifier	48
5.2.6.	Pixel assignment of various classes shown by confusion matrix relative to minimum distance classification	48
5.3.1	User accuracy and producer accuracy (in percent) estimates relative to parallelepiped classification	49
5.3.2	Pixel assignment of various classes shown by confusion matrix relative to parallelepiped classification	49
5.3.3	User accuracy and producer accuracy (in percent) estimates relative to minimum distance classification	49
5.3.4	Pixel assignment of various classes shown by confusion matrix relative to minimum distance classification	50
5.3.5	User accuracy and producer accuracy (in percent) estimates relative to minimum distance classification	50
5.3.6	User accuracy and producer accuracy (in percent) estimates relative to minimum distance classification	50
5.4.1	User accuracy and producer accuracy (in percent) estimates relative to parallelepiped classification	52
5.4.2	Pixel assignment of various classes shown by confusion matrix relative to parallelepiped classification	53
5.4.3	User accuracy and producer accuracy (in percent) estimates relative to minimum distance classification	53
5.4.4	Pixel assignment of various classes shown by confusion matrix relative to minimum distance classification	53

5.4.5	User accuracy and producer accuracy (in percent) estimates relative to minimum distance classification	54
5.4.6	User accuracy and producer accuracy (in percent) estimates relative to minimum distance classification	55



## CHAPTER 1: INTRODUCTION

### 1.1 Background Study

Remote Sensing utilize the microwave, infra-red, visible and region of the EM spectrum. The visible and infra-red regions are contemplated as optical regions and the microwave region is considered as non-optical region [1]. Systems working in the region of optical are being used for decades now, and thereby, are more advanced and hugely employed. Although, their utilization is confined by available sunlight and interference of the conditions of environment such as cloud cover and haze particularly in the tropical regions. So microwave remote sensing is preferred in such areas.

RADAR implies Radio Detection and Ranging. With their large geographical coverage and relatively high frequency, such systems offer attractive possibilities for various applications [2]. Active radar remote sensing technology is not constrained only to day time because it uses its own source of energy to light up the target. Radar wave is not disturbed much by environmental conditions and also provides a different perspective on the earth surface in comparison to what is provided by optical sensors as it is susceptible to the surface parameters like dielectric constant, roughness, and moisture content. Advanced Radar Systems such as Interferometric SAR, Differential Interferometric SAR and Polarimetric SAR, have improved the data retrieval capabilities of Radar.

The radar system uses an antenna to send a radar signal in side facing direction with respect to the path of flight, towards the earth and record the backscattered signal from the earth surface. In a Real Aperture Radar System, where aperture is an antenna, the amplitude of the return signal is recorded. The resolution of these systems is directly proportional to the antenna's length. As it is not pragmatic to use a very long physical antenna to improve the resolution, so Synthetic Aperture Radar systems were developed which can synthesize a long physical antenna using modified data recording techniques [3].

A procedure that use the remotely sensed image data to produce maps and/or tables showing the location and extent of various selected land cover types or earth surface feature is called Image classification [4]. Image classification is an important part of the remote sensing, image analysis and pattern recognition. Land use–land cover(LULC) information is valuable because it can be obtained regularly even across vast regions such as Urban region, Water region, natural forests, where field surveys are difficult to conduct. Quantitative assessment of land cover is required for every country in order to make proper planning against earth surface alteration, since land cover change is related to global change due to its interaction with climate, ecosystem process, bio-geochemical cycles, biodiversity and human activity. Remote sensing plays an important role in land cover classification. Since 1980's, radar polarimetry, i.e., the utilization of complete electromagnetic vector wave information, has been gaining more and more recognition from many researchers. Since then, radar polarimetry has been used in conjunction with remote sensing, and splendid results have been achieved. Cloud and Pottier [5, 6] made important contribution in the field of target decomposition by introducing the concept of Anisotropy, Entropy and alpha, and these parameters have become the standard tool for target characterization and have been used as the basis for the development of new classification methods introduced for the analysis of polarimetric data. There are mainly two groups of classification techniques that are supervised and unsupervised. Although much research has been done in the field of SAR image classification, there are certain limitations in each classification technique due to their problem specific nature. For example, besides being widely applicable the major disadvantage of supervised classification technique is that it is a single discriminative classifier which is applied to the individual pixel level or image objects (group of adjacent, similar pixels). If during training process any pixel is unidentified then supervised classifier cannot assign it to any class. Also supervised classifier finds it unable to recognize and represent unique categories not represented in training data. Unsupervised classification also suffers from certain limitations and disadvantages. One of the major disadvantages of unsupervised classification is that natural grouping obtained as a result of iterations in classifier does not necessarily correspond nicely to desired informational classes, and analyst has limited control over the classes chosen by the classification process [7, 8]. Thus in order to achieve more accurate results for land cover classification it is advantageous to opt for more advance classifier. Another objective of this dissertation is to improve our understanding about supervised

classification to see, how they interact with training data, and how they affect cluster labeling for land cover classification, if input parameters are SAR observables obtained by decomposition methods. The various methods are available for target decompositions for the identification of scattering characteristics. These are based on the study of polarimetric matrixes. There exists two main category of decomposition method 1) coherent decompositions 2) incoherent decompositions. The coherent decompositions describe measured scattering matrix through the radar in the form of simpler responses (Pauli, Krogager, Cameron decompositions etc). These decompositions methods exist only in case of point's scatter or pure targets. If speckle noise is present and a specified pixel belongs to distributed scatters then in such cases, incoherent technique is preferable for data processing. This technique has capability to use the conventional averaging and statistical methods. Incoherent decompositions work on polarimetric coherency matrix and also covariance matrix, such as the Freeman[9], The Four component[10], The Huynen[6], The Barnes[6] and the Cloude[5] decompositions. However, these kinds of conventional techniques try to relate each decomposition component with a particular scattering mechanism, invalidating their uses for different types of PolSAR images. In this thesis work we have worked only on model based decomposition techniques. In the present thesis, three supervised classification methods, namely minimum distance, maximum likelihood and parallelepiped, are used to critically analyze the classification based on Model based decomposition techniques.

## **1.2 Introduction to Polarization**

Polarization is a critical property of EM wave. An electromagnetic wave consists of two time-varying components, first electric field component and second magnetic field component, which are perpendicular to each other and also to the direction of propagation of EM wave. It can be described as the orientation of the electric field component, in a plane perpendicular to the direction of wave propagation. As the magnetic field is always orthogonal to the electric field, hence only the latter is used for defining the polarization of an EM wave.

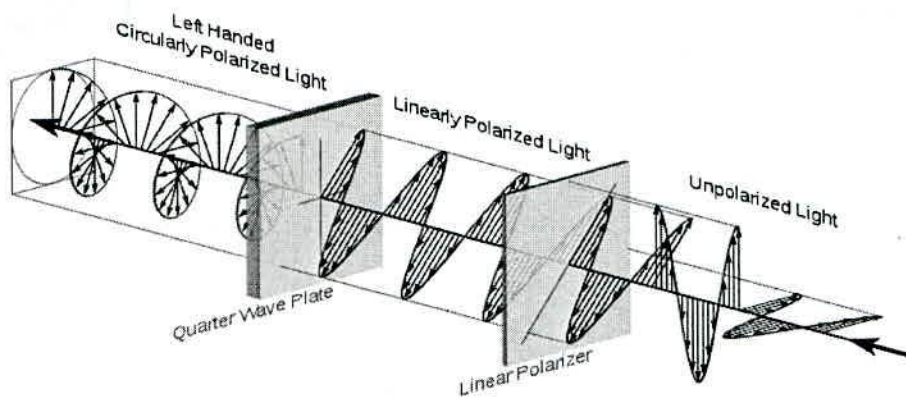


Fig1.1: Polarized and un-polarized of Propagation electromagnetic wave [11]

The green and blue wave as shown in Fig. 1-1 represents the vertical and horizontal components of the electric field, respectively. These components add up to form the total electric field vector as shown by the red wave. The electric field vector of a fully polarized wave draws out a regular pattern, when it is visualized in the direction of propagation of wave, which is known as polarization ellipse.

A polarization ellipse can be characterized in terms of the amplitude, ellipticity and orientation of the wave. The wave amplitude is given by electric field vector's length and the wave frequency is given by vector's rate of rotation. As shown in the figure, a polarization ellipse is given by a semi-minor axis with the length of  $b$  and semi-major axis with a length of  $a$ . Here,  $\vec{E}$  represents the electric field vector,  $E_y$  and  $E_x$  are the vertical and horizontal components of electric field. The angle formed by the major axis of the ellipse, measured anti clockwise from the direction of positive horizontal axis on incident plane is known as orientation angle  $\psi$  of the EM wave, which ranges from  $0^\circ$  to  $180^\circ$ . Ellipticity is a shape parameter, which is given by the angle  $\chi$  that varies from  $-45^\circ$  to  $+45^\circ$ . It also describes the degree of oval of the shape of the ellipse. The magnitudes and the phase difference between two components of electric field vector also control the shape of the polarization ellipse drawn out by it. Based on the ellipticity and orientation, polarisation can be categorized into elliptical, circular and linear. In linear polarisation, two components of electric fields are in phase, orientation is  $45^\circ$  and ellipticity is zero. When relative phase is increased to  $\pi/2$  radians and ellipticity is increased to  $\pi/4$  radians with orientation same at  $\pi/4$  radians, polarisation is called as circular polarisation. Rest of all is considered as case of elliptical polarisation [12].

A Synthetic Aperture Radar (SAR) system records both the amplitude and the phase of the back-scattered radiation by illuminating a scene with microwaves. In this way SAR makes a coherent imaging process. The initiation of SAR sensors direct to the idea of radar polarimetry. For forming the image, the received signal is sampled then it is converted into a digital image. Merging of radar technological concept and the primary assets of transverse nature of EM waves is called Radar polarimetry. Radar polarimetry is the science of analysing, processing and acquiring the polarization state of an Electromagnetic field [12].

Fully polarimetric SAR has four channels to acquire the whole scattering matrix, in which the signal is transmitted and received in two orthogonal polarizations. With the help of polarimetric radars it is become easy to get maximum information available than other conventional radars because of its preservation of phase term. The amalgamation of coherent polarimetric amplitude and coherent polarimetric phase into radar signal and image processing promises to bring about further improvements in monitoring capabilities in SAR image analysis. The magnitude information, along with its conventional phase data, can be utilized to learn the scattering mechanisms and determine the problems about the source of scattering [13]. This unique characteristic of polarimetric imaging radar makes it a powerful tool for land cover classification. The possible reasons which make polarimetric SAR a useful tool to characterize various targets of ecosystem for classification are mentioned below:

1. SAR being an active sensor is a day light acquisition system (unlike optical sensors).
2. Most of the radar sensors exhibit all weather capability. It is seen that characteristics of atmospheric such as smoke, haze, light rain, and cloud has little effect on the capacity of RADAR data acquisition system as atmosphere attenuation is minimum for wavelengths less than three centimeter [14].
3. SAR is not only sensitive to the relative proportion and distribution of various scatterers within an area-extended target but also sensitive to the physical, geometric and dielectric effects of different land cover types.
4. SAR not only provides ground surface information but can also be used for obtaining information beneath the ground (for certain moisture value and ground density) due to its capability to penetrate into soil and vegetation canopy.

Classification technique is a significant step towards the recovery of bio-geophysical parameters. This scheme is straight based on polarimetric SAR data is very much essential to appreciate the properties of the Earth surface, mostly for the physical estimation of scatterers. Thus Polarimetric SAR images are widely used for terrain classification as they can extract geometrical properties (size, shape, orientation distribution and spatial arrangement of objects) and physical information about the target like symmetry, non symmetry or irregularity of the target [14]. The present work is dedicated to the task of terrain classification of polarimetric PALSAR (Phased Array L- band Synthetic Aperture Radar) data by using various classification techniques. Classification of SAR images is required for various environmental and socioeconomic applications like agriculture monitoring, flood mapping, oil spill detection etc. Classification of image is done to identify different spectral classes present in it and their relation to some specific ground cover type. Classifying remotely sensed data into a thematic map is very challenging because it depends upon many factors, such as the complexity of the landscape in a study area, selected remotely sensed data. Also image processing and classification approaches, may affect the success of a classification.

### 1.3. Scattering, Covariance & Coherency Matrix

A radar wave of particular polarization, when interacts with the surface of target, experiences change in the state of polarization. The wave emitted from the surface of target after interaction will have response of horizontal polarization as well vertical polarization [15]. With regards to SAR polarimetry, this response from the backscattered wave in each polarization channel are stored in the form of 2 x 2 scattering matrix is given as

$$[S(HV)] = \begin{bmatrix} S_{HH} & S_{HV} \\ S_{VH} & S_{VV} \end{bmatrix} \quad (1.3.1)$$

Where all elements in the matrix performs the backscatter response of a target in the particular channel of polarization. The diagonal elements of the matrix shows the co-polarisation information, i.e. the transmitted and received radar wave have same polarization, and the off



diagonal terms shows the cross-polarisation information, i.e. the transmitted and received radar wave have polarization orthogonal to each other. The scattering matrix describes the information of the pure target exhibiting a particular scattering mechanism. However in general, the earth features are more complex or distributed demonstrating a variety of scattering response. In such case, the information obtained from the scattering matrix is insufficient to describe the physical properties of the surface. Therefore, the second order statistics of the scattering matrix – covariance and coherency matrix, are utilized for this purpose. These matrices are obtained from the scattering matrix by using its vectorized form derived from Pauli and Lexicographic basis [16]. The lexicographic vector form assuming the reciprocity condition  $S_{HV} = S_{VH}$  for mono-static case is given by

$$[K_l] = \begin{bmatrix} S_{HH} \\ \sqrt{2}S_{HV} \\ S_{VV} \end{bmatrix} \quad (1.3.2)$$

The covariance matrix is obtained as  $[c] = \langle [K_l]^* [K_l]^+ \rangle$  which is expressed as

$$[C] = \begin{bmatrix} S_{HH}S_{HH}^* & \sqrt{2}S_{HH}S_{HV}^* & S_{HH}S_{VV}^* \\ \sqrt{2}S_{HV}S_{HH}^* & 2S_{HV}S_{HV}^* & \sqrt{2}S_{HV}S_{VV}^* \\ S_{VV}S_{HH}^* & \sqrt{2}S_{VV}S_{HV}^* & S_{VV}S_{VV}^* \end{bmatrix} \quad (1.3.3)$$

Similarly, the coherency matrix is obtained as  $[T] = \langle [K_p]^* [K_p]^+ \rangle$ , where  $\langle \rangle$  represents the average over the whole data,  $K_p$  represents the Pauli vector given by

$$[K_p] = \begin{bmatrix} S_{HH} + S_{VV} \\ S_{HH} - S_{VV} \\ 2S_{HV} \end{bmatrix} \quad (1.3.4)$$

The coherency matrix obtained from above is given by

$$[T] = \begin{bmatrix} T_{11} & T_{12} & T_{13} \\ T_{21} & T_{22} & T_{23} \\ T_{31} & T_{32} & T_{33} \end{bmatrix} \quad (1.3.5)$$

$$\begin{aligned}
\text{Where } T_{11} &= \langle |S_{HH} + S_{VV}|^2 \rangle \\
T_{12} &= \langle (S_{HH} + S_{VV})(S_{HH} - S_{VV})^* \rangle \\
T_{13} &= 2\langle S_{HV}^*(S_{HH} + S_{VV}) \rangle \\
T_{21} &= T_{12}^*, \quad T_{22} = \langle |S_{HH} - S_{VV}|^2 \rangle \\
T_{23} &= 2\langle S_{HV}^*(S_{HH} - S_{VV}) \rangle, \quad T_{31} = T_{13}^*, \quad T_{32} = T_{23}^* \\
T_{33} &= 4\langle |S_{VV}|^2 \rangle
\end{aligned} \tag{1.3.6}$$

#### 1.4. Motivation of Work

The capability of radar polarimetry for information on the physical properties of the surface has resulted in many creative applications in geosciences research and on environmental issues. The radar Polarimetry (Polar: polarization, Metry: measure) has capability to get the information about physical properties of earth surface. This is the science of analyzing, processing and acquiring an EM wave polarization state. It deals with vectorial nature of polarised EM wave. One of the main drivers of the need for constant monitoring of land use generally must be filed uncertainty climate predictions determined by the feedback between climate and changes in land surface processes. Certain key processes, including changing land cover, vegetation and activity seasonally changing biomass periods of freezing and thawing of the soil, the activity of the heat and moisture of the soil is generally retrieved from satellites. Radar images are particularly suitable for the land use monitoring in forested areas, mainly. Although it may be less sensitive to optical data tree species, but the radar image has lots of applications through the optical image. Using optical sensors is further complicated in the winter because the atmospheric correction becomes tougher and less reliable with decreasing elevation angle of the sun. Plus totally opaque clouds, other atmospheric artifacts, such as smoke, pollution aerosols, and various forms of cloud shadow effects affect the quality and ease of use of optical data. By contrast, the radar data can be acquired in each orbit of the satellite, regardless of weather conditions, which makes it ideal for applications requiring long time and regularly time series data with a continuing time separation between observations.

## **1.5. Objective of the thesis**

The main objective of this dissertation is to study and critically analyze the following decomposition methods for their fruitful applications and to understand the need of decomposition:

1. Freeman-Durden three component decomposition theorem.
2. Four component decomposition.
3. Four component decomposition with rotation of coherency matrix.
4. The new General 4-component Decomposition with special unitary coherency matrix.

The second objective of this thesis is to compute scattering contribution i.e. the pixel values from each of the decomposition results and compare. The third objective is critically compare the land cover classification by using three supervised classification (minimum distance, maximum likelihood and parallelepiped) techniques based on three model based decomposition techniques (Four component decomposition, Four component decomposition with rotation of coherency matrix, The new General 4-component Decomposition with special unitary coherency matrix) and performing the accuracy assessments on the various classifications to find out the best approach and to calculate the predictable level of accuracy.

## **1.6. Dissertation outline**

The dissertation on "Classification of land cover using model based decomposition techniques for PALSAR data" deals with examination of the application of multi-polarized data of ALOS-PALSAR for land cover and land use mapping. Over here mainly the application aspects of information has been analyzed.

There are six chapters in this dissertation report. Chapter 1 gives a brief introduction of Synthetic aperture radar, radar polarimetry and land cover classification. Chapter 2 deals with the literature review of research paper study gone through during this work. Chapter 3 discusses about the theoretical concepts of different types of model based decomposition techniques and different classification techniques. Chapter 4 describes about the algorithms and processing techniques involved in the classification of land cover. Chapter 5 discusses about the results and finally Chapter 6 gives the concluding remarks along with the future scope of work.

## 2. LITERATURE REVIEW

### 2.1. Radar Remote Sensing and SAR

Radar systems remote sensing applications use radio waves or microwave region in wavelength range of 1 mm to 1.3 m in the electromagnetic (considerably longer than that of visible region). The radar wave's penetration capability is a major property differentiating it from the optical waves. Because of this specific property only the radar waves penetrate through cloud cover, haze, smoke, and extreme weather conditions, and making it a good choice for the remote sensing of scenarios such as flood or forest fires or the tropical regions. The important fact is that with the increase in wavelength, the penetration capability of the radar also increases. Radar remote sensing bands used in practice according to their penetration capability (increasing order of their wavelengths) are listed in the table below.

Table 2-1 Wavelengths of various Radar bands used for remote sensing

BAND	Wavelength
Ka	0.75-1.10 c.m.
K	1.10-1.67 c.m.
Ku	1.67-2.40 c.m.
X	2.40-3.75 c.m.
C	3.75-7.5 c.m.
S	7.5-15.0 c.m.
L	15.0-30.0 c.m.
P	30.0-130 c.m.

The target features presence on the earth surface and their angular position and distance can be calculated by Radar systems which uses radio waves for identification. Transmission of signals with known phase, amplitude, wavelength, polarization and time reference are mainly

used for achieving these criteria. Radar transmitted signals properties get altered on interaction with the target surface, and therefore the signal with the altered properties is scattered back and is received by the radar system. These changes in properties are used for estimating the target surface [17][18][19] and form the basis of understanding in radars. Radar cross section (RCS) of a given target describes the amount of the extracted power by its surface from the incident radar. RCS has nothing to do targets physical cross-section but has got the dimensions of area. Targets scatter is assumed to be isotropic in nature for all kinds of targets. RCS is defined for isolated or discrete scatterers only. The concept behind SAR polarimetry is with the science of acquiring, processing and analyzing electromagnetic wave polarization state. The description of scattering and propagation phenomena requires the wave polarization concept which can be given completely by their vector characterization property. The antennas design in complex radar systems are designed such that the EM waves are transmitted and received in more than single polarization [20]. The earth feature after reflecting the radio waves under investigation can change the transmitted wave polarization state, so most of the Radar systems, at the same point of time, are designed to receive different polarization components. Some SAR systems issues of concern are speckle effects, complex interactions, the effect of surface roughness and topographic effects. SAR polarimetry, with some of its unique characteristics, has potential for illustrating some interesting earth features applications dealing with the biophysical and geophysical parameters. SAR polarimetry has been able to give good quality results[20] in some of the applications such as the soil moisture, biomass, surface roughness estimation, surface slopes, height of the vegetation, tree species as well as ice thickness estimation and monitoring of snow cover.

## **2.2. Use of Remote Sensing For Land Use and Land Cover Change**

Remote sensing yields useful information about images of the environment is defined as the use of electromagnetic radiation sensor to record which can be interpreted[21] (Paul J. Curran 1985). combination spatial analysis is one area where Remote sensing is being increasingly used. the Extraction of relevant information from remote sensing imagery are obtained using geographic information systems (GIS) databases, whereas periodic pictures of thematic and geometric characteristics of terrain objects, update GIS databases (Janssen, 1993 In Luis M. T. *et al.*, 2003) and improving our ability to detect changes are provided by remote sensing data. Both

geographic information systems (GIS) and remote sensing (RS) have been recognized as powerful and widely applied effective tools in detecting the spatiotemporal dynamics of land use and land cover (LULC). RS can provide monitoring land-use patterns and processes valuable multitemporal data to the researchers (Lambin et al., 2001) and GIS techniques are mainly used for the mapping and analysis of these patterns (Hualou et al., 2006).

The potential demonstration of the realistic computer visualizations (depicting the forested environments dynamic nature) was made by the merging of remote sensing, GIS and visualization techniques. Scientific visualizations aid in forest and environmental management decision making as a support tool and in landscape ecology in the process of study findings. While visualization methods and software to recreate natural landscapes have already been developed extensively, the potential for illustrating land cover temporal data change acquired from the real world (Matt *et al.*, 2004) is required area to be studied in detail.

One important method of understanding ecological dynamics, such as natural and human disturbances, ecological succession and recovery from previous disturbances, is the analysis of changing land cover patterns (Turner 1990). An excellent data source is the Satellite imagery and helps in performing landscape structural studies. The number, size and shape of patches (simple measurements of pattern), can indicate functionality of a land cover type more as compared to the total area of cover alone (Forman 1995). Fragmentation statistics are found to be useful in indicating the surrounding habitat resulting impact and describing land cover change type as they are compared across time. The comparison between images of areas of land cover change can also be to landscape characteristics for the determination whether change is more likely to occur in certain environmental and human induced factors presence. This classification detail level presents land cover change patterns analysis opportunities at a structural scale (Matt et al 2004).

The four main components of remote sensing system using electromagnetic radiation are : a source, interaction with atmosphere, interactions with Earth's surface and a sensor. The characteristics and amount of radiation emitted or reflected from the Earth's surface is entirely dependent upon the Earth's surface objects characteristics. Therefore, different Earth objects interact with radiation differently and fundamental issue on classification of satellite image (Paul J. Curran 1985) is the knowledge of this interaction. Therefore, based on this Earth surface

objects reflectance variation, it has been made possible the classification and distinguishing land use land cover.

Supervised or unsupervised procedures developed for a satellite image classification. Prior training areas specification by the analyst is required to be known and major land cover types are delimited manually in a supervised approach (a key for electronically classifying the image). study area knowledge is required in advance. no such visual interpretation, in contrast, is involved in the case of an unsupervised method. In order to derive a required number of land classes and their associated spectral signatures (Tudor G.J. *et al.*, 1998) automated methods are used to cluster reflectance values.

### **2.3. Polarimetric Decompositions**

The concept of polarimetric decomposition first came into light in work of Chandrashekhar on scattering of light by small anisotropic particles.[22][9][23]but Huygen was the first person to describe the main theory behind it. There is requirement for the description of multivariate statistical variables in the radar images target of interest due to the combination of random vector scattering effects and coherent speckle noise from various types of surfaces. Therefore, generation of average or dominant scattering mechanism concept came into picture for inversion or classification of the radar information. The theories behind objective of the polarimetric target decomposition is mainly to explain the average scattering mechanism as a combination of independent elementary scattering mechanisms to each component's association with the physical scattering mechanisms.

There are most importantly two target decomposition categories of theories those were developed during the past : Incoherent and Coherent target decompositions[22]. The complete classification of polarised scattering waves coherent target decompositions are described by Coherent schemes in which the scattering matrix completely describes the polarimetric information of the target.

Kimura et al. [24][25] in his paper has described the built-up areas polarisation shift angles. The three types of components which describe built-up areas scatterings are given by- single bounce scattering components generated by reflections from ground, roof or wall; double bounce scattering components generated by reflections from wall-ground pair; triple bounce scattering components generated by reflections from wall-ground-wall. The double bounce

scattering contribution is described by the phase difference between the HH and HV polarisations. In their paper they have taken care of increment of the surface bounce scattering and triple bounce scattering, due to which they have judged the lower absolute values of the orientation angles derived from X-band as compared to L-band. The orientation angle shifts affect the radar cross section of the effective scattering pixel area. The target rotation w.r.t. incident radar wave causes it to have a different RCS( i.e.to take into account for the incident wave extracted energy and it's isotropic re radiation) explained by the specific orientation's implicit area.

Iribe et al. [26] has described the shifts of the orientation angle in the case of urban areas and found out it's effects caused by the angle relation between the flight direction and the target rotation. The radar look direction even in the case of same target changed as according to the induced orientation angle shifts. The coherent nature of the targets is considered to be reliable because of the considerable reliable orientation angle shifts derived from the urban scatterers. Pauli, Krogager, Touzi and Cameron. Krogager have proposed a scheme on the complex Sinclair matrix i.e. for the coherent three component decomposition significantly associated to the coherent decompositions and describing mainly on the canonical scattering mechanisms [27], with Sphere, dipole, diplane and helix described as canonical objects. The thin wire or dipole target and the diplane have been described as a function of 2 variables i.e the orientation angle about the radar line of sight. The scattering matrix was decomposed into diplane, sphere and helix Polarimetric Decompositions according to these targets. [22][9][23].

On implementation of the rotated coherency matrix, a clear discrimination using 4component scattering model decomposition between vegetation and oriented urban structures was obtained. Earlier, the oriented urban structures were incorrectly decomposed into volume scattering component, were correctly decomposed using deorientation techniques into double bounce scattering component.

In [26] a polarimetric scattering model has been introduced for the purpose of fitting into urban areas. In this model, the applications of three types of elementary scattering mechanisms were introduced – even bounce, odd bounce and cross scattering. A moderately rough surface from the single bounce, triple bounce and Bragg's surface scattering has been modeled as odd bounce scattering model. The description of even bounce scattering model tells about dihedral



corner reflectors scatterings such as orthogonal pair of ground and wall. The cross scattering model describes about mainly the urban areas scattering components, which takes into account the cross-polarised components generated from the oriented thin wire targets and dihedral corner reflectors present in urban areas. Oriented street patterns have been known of generating cross-polarised response. The most beneficial part for discriminating urban features from the natural features is done with the help of the polarimetric correlation coefficients. X-band PiSAR data has been tried with the above mentioned technique in comparison with the Freeman three component scattering model. The model's accuracy is mainly dependent on the street pattern orientation. The dominant property of the even bounce scattering is found to be in urban areas.

Multiple Component Scattering Model as proposed by Zhang et al. [28] extends the four component scattering model by including a fifth component - wire scattering, mainly for polarimetric decomposition as in the case of eaves, observations from the edges and window frames present in the urban areas. The thin wire scatterer as described by the wire scattering is modeled by a function of the orientation angle around radar line of sight. Through the helix and the wire components the cross-polarised response gets affected. In urban structures, the double bounce, helix and wire scattering components were found to be predominant, especially for the case where the edge structures are parallel to the flight path. Both reflection symmetry and asymmetry conditions, as a general case, are represented and considered in this decomposition.

#### **2.4. Land Use Classification**

Several efforts in the past have been made of devising a land use system that provides completeness of data and lack of overlap, useful information to a wide variety of users and maintains principles such as, independence of observation tools and links with internationally recognized socio-economic classifications. Additionally it is required that the reference system classification should be independent of scale and independent of any of the data collection method used. According to FAO (1999), the functional and the sequential approaches are the two broad approaches which make efforts in the land use classification, and are described below.

- **Functional approach:** The functional approach has been found to be applicable for all land use purposes such as residential, agriculture, forestry, etc. and gives the land description in terms of its socio-economic purpose. So, land functional uses can be made at a single point of time or

over a shortened period of time. Several classification systems are making use of the functional approach.

- **Sequential approaches:** The sequential approach was mainly used for classifying agricultural lands and is often named to be sequence of operations approach. This approach defines the activity carried out by humans on land use approach, with the intention to obtain products and/or benefits through using land resources as a result of series of operations on land. By definition, this kind of approach requires a large no. of observations taken over period of time.

The data availability tells also about the mixed land use/land cover design of national land classification systems influences. Land use classification system has kept focus on agricultural lands in many countries, from which land use classification design becomes much easier. In fact, this has become the primary reason for the development of mixed systems. Natural land areas like forests and grasslands are easier to measure on a land cover basis while agricultural land and built-up areas are more easily defined on the basis of land use. So total land area classifications can typically be considered as mixed land cover/land use, it can be argued that most national land classification schemes are primarily pure land use systems because the focus has been on agriculture. FAO (1999), tells clearly the requirement for understanding of the difference between land cover and land use classification for the purpose of pure land use classification; and according to it land use and land cover classification differentiation is as follows:

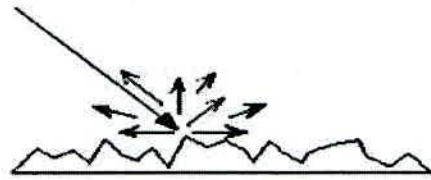
- **Land use classification** is based upon the actual purpose and the function being mostly dependent on the current use of land. Thus, it defines a series of activities undertaken for land use application to produce one or more goods or services. Same piece of land can be incurred with several land uses and also a given land use may take place on one, or more than one piece of land. Such classification of Land investigation to present the environmental and economic outcomes provides a quantitative measure of land in relation to the impacts of various natural events and human activities for future planning and precise and quantitative analysis. Such information is generally based on mapping of land area using techniques like aerial photography, cadastral surveys, etc. supported by ground truthing.

- **Land cover classification** is based on the earth's bio-physical cover surface observations irrespective of its uses including construction works, vegetation, ice, water, sand or bare rocks surface. Remote sensing obtains such information from ground surveys.

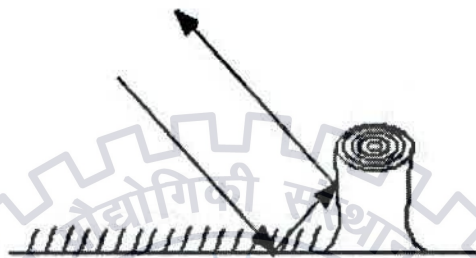
## CHAPTER 3: THEORETICAL CONCEPT

### 3.1. Polarimetric Decompositions

Various mathematical and physical models have been developed for extracting the target information from the backscatter. Most of these are forward models which are usually complex and employ large number of field based input parameters to model the backscatter and are difficult to invert to provide a unique solution [9]. Another category is the decomposition models, which are comparatively easier to understand and do not require a large number of input parameters. The polarimetric decomposition theorems were developed for extracting the physical information about the target surface. These techniques are aimed on separating the polarimetric measurements from a random media into independent elements which can be associated to the various physical scattering mechanisms occurring on the ground. These techniques are broadly classified into two categories- coherent and incoherent decompositions. In case of coherent decompositions, the scattering matrix is expressed as a weighted combination of scattering response of simple or canonical objects. These types of decompositions are applicable to only pure or coherent targets which give completely polarized backscatter. Many man-made structures are examples of such pure targets whereas the natural features are represented by the distributed targets, which give a complex scattering response due to presence of speckle noise. Therefore, these scatterers cannot be analyzed by exploiting the scattering matrix. For such scatterers, incoherent decompositions are employed which are aimed at separating the measured covariance or the coherency matrix as a combination of second order descriptors representing simple scattering mechanisms [29]. Different model based incoherent decompositions have been developed in past. Freeman and Durden gave a significant contribution to incoherent decompositions by proposing a three component scattering model. This model was developed for describing the polarimetric response from the natural distributed areas by considering three basic scattering mechanisms – single bounce or surface bounce, double bounce and volume scattering. The single or surface bounce scattering is modelled as first order Bragg's scattering. For a pair of orthogonal surfaces having different dielectric constants, such as ground and tree trunk or ground and wall, the modelled scattering represents double bounce. Volume scattering is modeled as the response from randomly oriented dipoles in a vegetation canopy [9][30].



(a) Surface scattering



(b) Double-bounce



(c) Volume scattering

Figure 3.1:(a) Surface scattering from a rough surface (b) Double bounce scattering from a ground and tree trunk (c) Volume scattering from multiple reflections from the tree branches[18]

## 3.2. Model Based Decomposition

### 3.2.1. Three component scattering model

From 1992 to 1998 freeman and durden developed a three-component scattering model which is suitable for classification and inversion of maximum utilization polarimetric SAR image information. The Freeman decomposition models the covariance matrix as the contribution of three scattering mechanisms:

- **Volume scattering:** Modelled by a set of randomly oriented dipoles.
- **Double-bounce scattering:** Modelled by scattering from a dihedral corner reflector.
- **Single-bounce scattering:** Modelled by a first-order Bragg surface scatterer.

The reflection symmetry condition, for natural distributed targets, states that the cross-correlation between the co-polarized and cross-polarized scattering elements is approximately of zero value which is used in Freeman and Durden decomposition [1]. In this method only 5 parameters are utilized however there exist 9 independent parameters. The coherency matrix is given as

$$\langle [T] \rangle = f_s \langle [T] \rangle_{\text{surface}} + f_d \langle [T] \rangle_{\text{double}} + f_v \langle [T] \rangle_{\text{volume}} \quad (3.1.1)$$

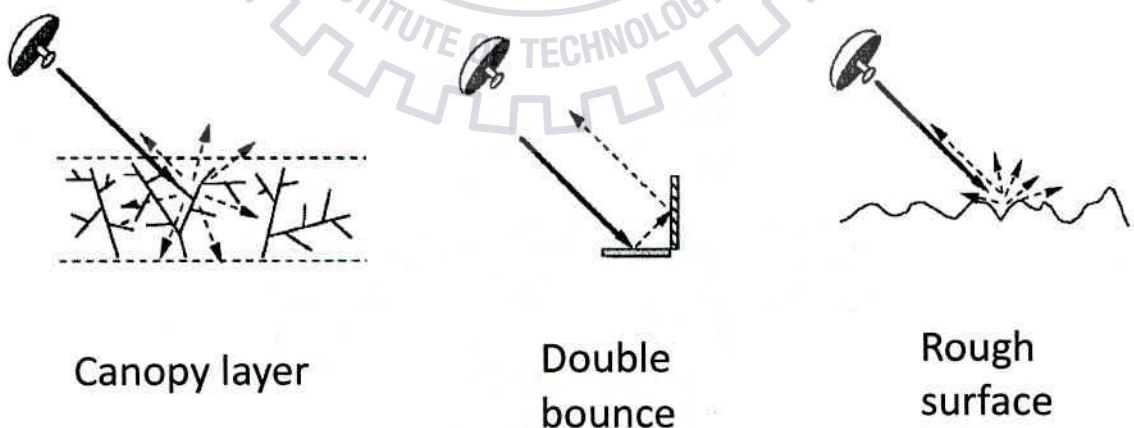


Fig 3.2: Sketch of three scattering mechanisms used in the model [9]

Assuming the three processes to be independent from one another, each contributes to the total observed coherency matrix [T] as

$$[T] = [T_s] + [T_D] + [T_V] \quad (3.1.2)$$

Where  $[T_s]$ ,  $[T_D]$  and  $[T_V]$  are the coherency matrices for the surface, dihedral and volume scattering respectively.

**a) Surface Scattering Contribution**

$$[T_s] = f_s \begin{bmatrix} \beta^2 & \beta & 0 \\ \beta & 1 & 0 \\ 0 & 0 & 0 \end{bmatrix} \quad (3.1.3)$$

**b) Dihedral Scattering Contribution**

In this case, the scattering is completely described by the Fresnel reflection coefficients of each reflection plane.

For example, the scattering matrix of a soil-trunk dihedral interaction is obtained as

$$[T_D] = f_D \begin{bmatrix} \alpha^2 & -\alpha & 0 \\ -\alpha & 1 & 0 \\ 0 & 0 & 0 \end{bmatrix} \quad (3.1.4)$$

**c) Volume scattering**

For volume scattering, it is assumed that the radar return is from a cloud of randomly oriented, very thin, cylinder-like scatterers.

$$[T_V] = f_V \begin{bmatrix} 1 & 0 & 0 \\ 0 & \delta & 0 \\ 0 & 0 & \delta \end{bmatrix} \quad (3.1.5)$$

Where,  $f_V$  is the backscattering amplitude and  $\delta$  depends upon the shape and the dielectric constant of the scatter. Its value is between 0 and 0.5, where the value 0 corresponds to spheres and 0.5 to dipoles. The Freeman decomposition presents 5 independent parameters  $\{f_v, f_d, f_s, \alpha, \beta\}$  and only 4 equations. Consequently, some hypothesis must be considered in order to find the values of  $\{f_v, f_d, f_s, \alpha, \beta\}$ .

- If  $f_s \beta > f_D \alpha \rightarrow \beta = 1$  : Dominant Surface Scattering
- If  $f_s \beta < f_D \alpha \rightarrow \alpha = -1$ : Dominant Dihedral Scattering

The scattering powers corresponding to surface, double and volume scattering component is given by

$$P_s = f_s(1+|\beta|^2) \quad (3.1.6)$$

$$P_d = f_d(1+|\alpha|^2) \quad (3.1.7)$$

$$P_v = 8 * f_v / 3 \quad (3.1.8)$$

### 3.2.2. The original Four-component decomposition: Y40

Although three component decomposition methods was applied to tropic forest classification effectively, since the cross-pol components are not roughly equal to zero in complex urban areas, so its non-reflection symmetric assumption is not completely fulfilled. For avoiding such constrain, Yamaguchi et al. [10] added one more component that is helix scattering which became the fourth component to the decomposition. This method uses six parameters out of nine in the coherency matrix and leaving three parameters unaccounted. The coherency matrix can be defined as

$$\begin{aligned} \langle [T] \rangle &= f_s \langle [T] \rangle_{\text{surface}} + f_d \langle [T] \rangle_{\text{double}} + f_v \langle [T] \rangle_{\text{volume}} + f_c \langle [T] \rangle_{\text{helix}} \\ &= f_s \begin{bmatrix} 1 & \beta^* & 0 \\ \beta & |\beta|^2 & 0 \\ 0 & 0 & 0 \end{bmatrix} + f_d \begin{bmatrix} |\alpha|^2 & \alpha & 0 \\ \alpha^* & 1 & 0 \\ 0 & 0 & 0 \end{bmatrix} + 0.25f_v \begin{bmatrix} 2 & 0 & 0 \\ 0 & 1 & 0 \\ 0 & 0 & 1 \end{bmatrix} + 0.5f_c \begin{bmatrix} 0 & 0 & 0 \\ 0 & 1 & \pm j \\ 0 & \pm j & 1 \end{bmatrix} \end{aligned} \quad (3.2)$$

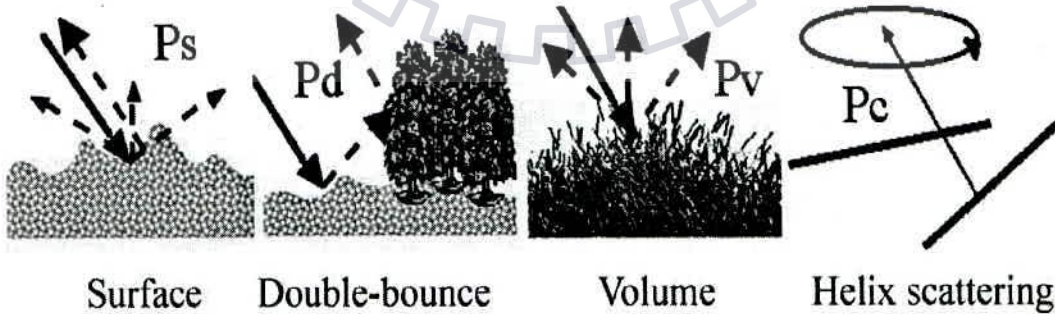


Fig 3.2: Sketch of four scattering mechanisms used in model [10]

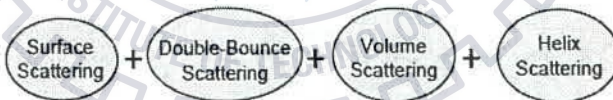
### 3.2.3. Yamaguchi 4-CSPD with rotation of coherency matrix: Y4R

In the imaging process, sometimes we face the problem of occurrence of negative power and problem in differentiating oriented urban area vs vegetation area due to their similar polarimetric responses. The high value of HV component is the main cause of these problems. These problems can be handled efficiently by minimizing the cross-polarized term  $T_{33}$  through a rotation of matrix [31] which is straight forward associated with avoidance of negative power occurrence. This method accounts six parameters out of eight in the coherency matrix and leaving two parameters unaccounted. The coherency matrix rotation by an angle  $\theta$  around the radar line of sight is given by

$$\langle T(\theta) \rangle = [R(\theta)] \langle T \rangle [R(\theta)] = f_s \langle T(\theta) \rangle_{\text{surface}} + f_d \langle T(\theta) \rangle_{\text{double}} + f_v \langle T(\theta) \rangle_{\text{volume}} + f_c \langle T(\theta) \rangle_{\text{helix}}$$

$$\text{where } R(\theta) = \begin{bmatrix} 1 & 0 & 0 \\ 0 & \cos 2\theta & \sin 2\theta \\ 0 & -\sin 2\theta & \cos 2\theta \end{bmatrix} \quad (3.3.1)$$

$$\text{and } \theta = 0.24 * \tan^{-1} \frac{2 * \text{Re}[T_{23}]}{T_{22} - T_{33}} \quad (3.3.2)$$



$$\begin{bmatrix} 1 & \beta^* & 0 \\ \beta & |\beta|^2 & 0 \\ 0 & 0 & 0 \end{bmatrix} + \begin{bmatrix} |\alpha|^2 & \alpha & 0 \\ \alpha & 1 & 0 \\ 0 & 0 & 0 \end{bmatrix} + \frac{1}{4} \begin{bmatrix} 2 & 0 & 0 \\ 0 & 1 & 0 \\ 0 & 0 & 1 \end{bmatrix} + \frac{1}{2} \begin{bmatrix} 0 & 0 & 0 \\ 0 & 1 & \pm j \\ 0 & \mu j & 1 \end{bmatrix} + \frac{1}{30} \begin{bmatrix} 15 & 5 & 0 \\ 5 & 7 & 0 \\ 0 & 0 & 8 \end{bmatrix}$$

$$(3.3.3)$$



where Rotation coherency matrix elements are

$$T_{11}(\theta) = T_{11}$$

$$T_{23}(\theta) = j\text{Im}(T_{23}), T_{32}(\theta) = -j\text{Im}(T_{23})$$

$$T_{12}(\theta) = T_{12} \cos 2\theta + T_{13} \sin 2\theta, T_{21}(\theta) = T_{12}^*(\theta)$$

$$T_{13}(\theta) = -T_{12} \sin 2\theta + T_{13} \cos 2\theta, T_{31}(\theta) = T_{13}^*(\theta)$$

$$T_{22}(\theta) = T_{22} \cos^2 2\theta + T_{33} \sin^2 2\theta + \text{Re}(T_{23}) \sin 4\theta$$

$$T_{33}(\theta) = T_{33} \cos^2 2\theta + T_{22} \sin^2 2\theta - \text{Re}(T_{23}) \sin 4\theta.$$

(3.3.4)

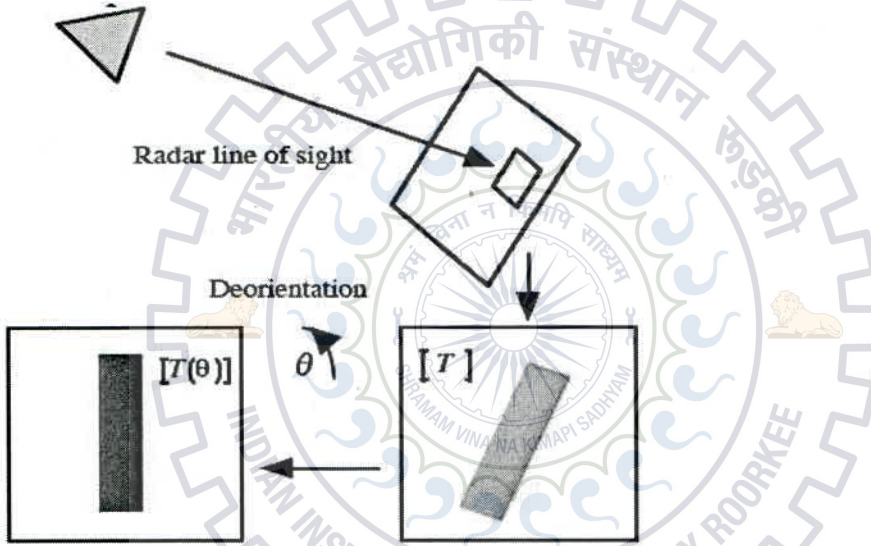


Fig 3.3: Sketch of four scattering mechanisms with rotation of theta angle to Coherency matrix [31]

### 3.2.4. New General 4-CSPD with Unitary Transformation (G4U)

The new general four-component decomposition method [32] is addressed through the use of a special matrix transformation (unitary transformation) to rotated coherency matrix. Although there is no change in the information of coherency matrix after unitary transformations so to eliminate the  $T_{23}$  element the rotated coherency matrix can be transformed by a special matrix transformation (unitary transformation) without any change in the information. This new method provides the decrease in the number of polarization parameters from eight parameters to seven parameters with considering the  $T_{13}$  element. Finally with this method seven polarimetric parameters out of seven are utilized. It has been validated that G4U method gives the more

accurate result as compared to the existing four-component decomposition and original three - component decomposition methods. A second unitary transformation can be defined such as

$$[T(\varphi)] = [R_p(\varphi)] [T(\theta)] [R_p(\varphi)] =$$

$$f_s \langle [T(\varphi)] \rangle_{\text{surface}} + f_d \langle [T(\varphi)] \rangle_{\text{double}} + f_v \langle [T(\varphi)] \rangle_{\text{volume}} + f_c \langle [T(\varphi)] \rangle_{\text{helix}} \quad (3.4.1)$$

The surface scattering model, the expansion matrix becomes

$$\langle [T(\varphi)] \rangle_{\text{surface}} = [U(\varphi)] \langle [T] \rangle_{\text{surface}} [U(\varphi)]^\dagger = \begin{bmatrix} 1 & \beta^* \cos 2\varphi & -j\beta^* \sin 2\varphi \\ \beta \cos 2\varphi & |\beta|^2 \cos^2 2\varphi & -j|\beta|^2 \frac{\sin 4\varphi}{2} \\ j\beta \sin 2\varphi & j|\beta|^2 \frac{\sin 4\varphi}{2} & |\beta|^2 \sin^2 2\varphi \end{bmatrix} \quad (3.4.2)$$

The double bounce scattering model, the expansion matrix becomes

$$\langle [T(\varphi)] \rangle_{\text{double}} = [U(\varphi)] \langle [T] \rangle_{\text{double}} [U(\varphi)]^\dagger = \begin{bmatrix} |\alpha|^2 & \alpha \cos 2\varphi & -j\alpha \sin 2\varphi \\ \alpha^* \cos 2\varphi & \cos^2 2\varphi & -j \frac{\sin 4\varphi}{2} \\ j\alpha^* \sin 2\varphi & j \frac{\sin 4\varphi}{2} & \sin^2 2\varphi \end{bmatrix} \quad (3.4.3)$$

The helix scattering model, the expansion matrix becomes

$$\langle [T(\varphi)] \rangle_{\text{double}} = [U(\varphi)] \langle [T] \rangle_{\text{double}} [U(\varphi)]^\dagger = \frac{1}{2} \begin{bmatrix} 0 & 0 & 0 \\ 0 & 1 \pm \sin 4\varphi & \pm j \cos 4\varphi \\ 0 & \mp j \cos 4\varphi & 1 \pm \sin 4\varphi \end{bmatrix} \quad (3.4.4)$$

Due to cross-polarized HV component, we divided volume scattering model into four cases.

$$\langle [T(\varphi)] \rangle_{\text{volume}} = [U(\varphi)] \langle [T] \rangle_{\text{volume}} [U(\varphi)]^\dagger = 0.25 * \begin{bmatrix} 2 & 0 & 0 \\ 0 & 1 & 0 \\ 0 & 0 & 1 \end{bmatrix} \quad (3.4.5)$$

For dipole scattering with probability density function of  $P(\theta) = \frac{1}{2\pi}$ ,

$$\langle [T(\varphi)] \rangle_{\text{volume}} = \frac{1}{30} \begin{bmatrix} 15 & -5 \cos 2\varphi & j5 \sin 2\varphi \\ -5 \cos 2\varphi & 7 + \sin^2 2\varphi & j \frac{\sin 4\varphi}{2} \\ -j5 \sin 2\varphi & -j \frac{\sin 4\varphi}{2} & 7 + \cos^2 2\varphi \end{bmatrix} \quad (3.4.6)$$

For dipole scattering with probability density function of  $P(\theta) = \frac{1}{2} \cos 2\theta$ ,

$$\langle [T(\varphi)] \rangle_{\text{volume}} = \frac{1}{30} \begin{bmatrix} 15 & 5 \cos 2\varphi & -j5 \sin 2\varphi \\ -5 \cos 2\varphi & 7 + \sin^2 2\varphi & j \frac{\sin 4\varphi}{2} \\ j5 \sin 2\varphi & -j \frac{\sin 4\varphi}{2} & 7 + \cos^2 2\varphi \end{bmatrix} \quad (3.4.7)$$

For dipole scattering with probability density function of  $P(\theta) = \frac{1}{2} \sin 2\theta$ ,

$$\langle [T(\varphi)] \rangle_{\text{volume}} = \frac{1}{30} \begin{bmatrix} 0 & 0 & 0 \\ 0 & 7 + \sin^2 2\varphi & j \frac{\sin 4\varphi}{2} \\ 0 & -j \frac{\sin 4\varphi}{2} & 7 + \cos^2 2\varphi \end{bmatrix} \quad (3.4.8)$$

For oriented dihedrals centred around 0 degree.

### 3.3. Classification Schemes

Each and every nation has been using land cover Quantitative analysis and it has become essential in formulating and planning next to earth surface change, as land cover change happens due to its interaction with climate, biodiversity, bio-geochemical cycles, human activity and eco system process and is therefore linked to global change. The socioeconomic and environmental applications are like mapping of monitoring of agriculture, oil spill detection, flood, etc. Classification assessment of SAR images plays a vital role. Classification of land cover which is a significant part of remote sensing requires to be done so as to ease accessibility of different SAR images through RADARSAT, ENVISAT, and ALOS PALSAR etc.

**Classification Technique-** In this Technique, we assign specified pixel data elements set to some classes through which data elements assigning is done at reduced cost [34]. The classification method's main purpose is to classify all pixels in image into one of several land cover classes. This categorized data may then be utilized to make contemporary maps of the land cover present in an image. More or less classification association with many factors like remotely sensed data, selected image processing, classification approaches, etc. makes the Classification of land cover through remotely sensed data very demanding. The following are the main steps involved in classification [33]:

1. Appropriate classification system Determination required.
2. Feature extraction through Image pre-processing.
3. Training samples Selection.
4. Suitable classification method selection.
5. Post classification and accuracy assessment.

Classification methods are mainly of two types: supervised and unsupervised. In Supervised techniques, the user is required to "train" the gathered samples to teach the classifier and find out the feature space decision boundaries, and size of samples utilized and properties to train the classifier appreciably affect these decision boundaries. In Unsupervised classifiers, we try to "learn" the characteristics of every class (and input data possibly tells even the no. of classes directly).

### ***Parallelepiped Classification***

The parallelepiped classifier accompanies each and every class by collection of probable values on every band. The range is determined by maximum and minimum pixel values in a particular class or just by a particular selection of standard deviations on both side of mean of training data for a certain class. These kinds of decision boundaries form n-dimensional parallelepiped. Assuming a pixel value can be found above the minimal threshold and below the maximum threshold and it will be allocated to that class. Whenever the pixel value lies in numerous classes, the pixel is allocated to the previous class matched or even overlaps class. In cases where the pixel fails to fall within any one of the parallelepiped classes it will be chosen as unclassified or even null class. The benefit of this approach is the fact that it is extremely straightforward to execute while in contrast capabilities wise it is really substandard, and then for correlated data there might be overlap of the parallelepipeds because their sides are parallel to the spectral axes. Subsequently, you will discover certain data that can never be distinguished [35][36]

### ***Minimum Distance Classification***

The decision rule adopted by the minimum distance classifier to determine a pixel's label is the minimum distance between the pixel and the class centers (mean), measured either by the Euclidean

Distance or the Mahalanobis generalized distance. Classification is then performed by placing a pixel in the class of the nearest mean [36]. The advantage of this classifier is that it not only is a mathematically simple and computationally efficient technique, but also provides better accuracy than maximum likelihood procedure, in the case when the number of training samples is limited. But the shortcoming is that by characterizing each class by its mean reflectance only, minimum distance classifier has no knowledge of the fact that some classes are naturally more variable than others, which consecutively can lead to misclassification.

### ***Maximum Likelihood Classification***

The MLC procedure is based on Bayesian probability theory. Decision rule is decided by calculating mean and standard deviation of each training set and deriving probability density

function from mean and standard deviation for computing probability of each pixel belonging to each class. The classifier then assigns pixel to the class for which the probability is the highest. It yields higher accuracy than other classifiers. It has some demerits like: (i) It is computationally intensive and time consuming technique; (ii) Each data sample has to be tested against all classes in a classification, which leads to relative degree of inefficiency; (iii) With a fixed relatively small size training set the classification accuracy may actually decrease when the number of features is increased.[36].



## CHAPTER 4: MATERIAL AND METHODOLOGY

In this chapter methodology adopted for polarimetric analysis of SAR images for classification of land cover is discussed. Starting with the discussion of study site used in our dissertation work, we have discussed about the SAR images used for land cover classification. Model based decomposition theorems which form the basis for classification are discussed next followed by various classification techniques.

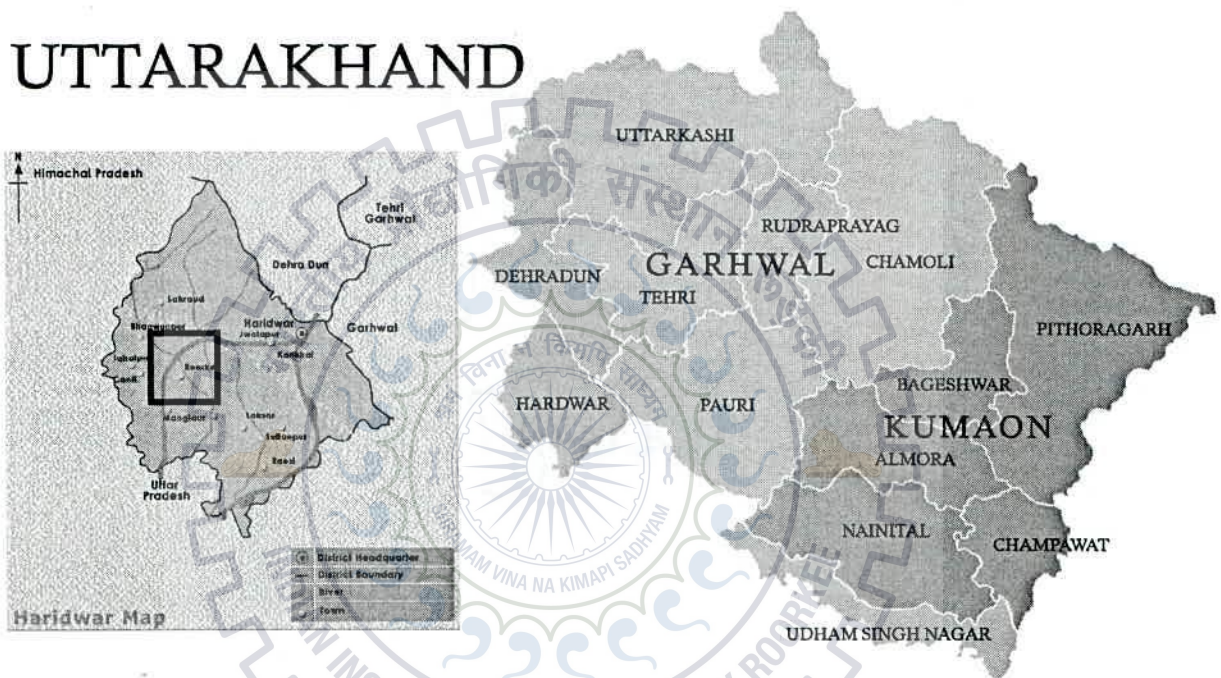


Figure-4.1: Study area location

In this particular chapter, the data set used and the software tools used in the study are explained in the 1<sup>st</sup> part. The following part explains in detail the methodology used to achieve the objective of the research presented. The overall methodology adopted for this research was presented in Figure 4.1

### 4.1. Study Area

The study area chosen for this research is situated in the state of Uttarakhand in southwestern part of India. It has centre latitude  $29.61380^{\circ}$  and longitude  $78.0086730^{\circ}$ . The south western part of the image contains urban area, large land area, Ganga canal which comes from Haridwar city, Solani river and small forest region. The major urban areas that fall in this study area are

Roorkee, Laksar, Bijnor regions. In general, these urban areas contained randomly distributed in addition to human settlements and also agricultural vegetation patches. The footprint of the data in the study area is presented in Figure 4.1.

#### 4.2. Data Used

ALOS PALSAR L-band fully polarimetric SLC data has been utilized in this study. The ALOS (Advanced Land Observing Satellite) is one of the largest Japanese satellite PALSAR (Phase array L-Band Synthetic Aperture Radar), one of 3 remote sensing instruments onboard ALOS, was jointly established by the Japan Exploration Agency Aerospace (JAXA) and Japan Organization Resources Observation System (BIRDS). The description of the data set is provided in Table 4-1. The L-band fully polarimetric data was in SLC level format (single look complex) 1.1, in which each pixel in the image contains a complex value, which contains the amplitude and phase related to the response of polarization dispersion of scatterers represented by a single SAR resolution cell. The dataset comprised four image files in SLC format (. SLC) for each polarization channel. (HH, HV, VH and VV). The ALOS PALSAR product is level 1.1 data in JAXA-CEOS format, which is single look complex data on slant range. The product has single number of looks on range and azimuth.

Table:4.1:-Data set information

<b>Characteristics of Dataset</b>	
Sensor	ALOS/PALSAR
Product	L-1.1
Date	11 April 2011
Polarisation	HH+HV+VV+VH
Incidence Angle	25.8°
Ground Pixel Resolution (Range)	3.792 M
Ground Pixel Resolution (Azimuth)	18.737 M
Nadir angle (or LOOK angle)	21.5°



### 4.3. SOFTWARE USED

In the whole study, 5 Software are used:

- **ENVI 4.7** - *Environment for Visualizing Images (ENVI)* was for processing SAR images.
- **SARSCAPE 4.1**- SARSCAPE data analysis module allows image processing with ENVI. This software complements ENVI's functionality for analyzing perfectly and remote sensing data visualization of any kind.
- **MATLAB 2010**- This software was used for developing algorithms of various decompositions and for plotting various graphs.
- **POLSAR PRO.**
- **NEST.**

### 4.4. Methodology

In this particular study, the method used is based on the use of the coherency matrix of polarization as it is very sensitive to the orientation of the scatterers and is closely associated with physical scattering mechanisms that occur on the surface of the target. As the data set was available in the SLC format, therefore the first step was to transform the dataset into a standard format and extract the elements of the coherency matrix by using POLSAR PRO software. Preprocessing was conducted to convert the data from slant range to ground range using the multilooking process. From the multi looked data the coherency matrix elements were extracted. The second step was the terrain correction. Third step involved the use of ENVI 4.7 software to convert the “.hdr” to “.txt” files of all element of the coherency matrix. In the fourth step, the four different decomposition algorithm using Multiple Component Scattering Model was developed by using the software MATLAB 2010 for getting different scattering power matrix. The detailed mathematical modeling of the decomposition algorithm has been described in the next section. In fifth step the results from all four types of decomposition methods i.e. Freeman decomposition, the original four component decomposition, four component decomposition with rotation of coherency matrix and new general four component decomposition techniques were compared and analyzed. In the last part three supervised classification algorithms (Parallelepiped, Minimum distance, and Maximum likelihood) are applied over polarimetric observables obtained by decomposition techniques. The classification tests based on the parameters obtained by three D decomposition, four component decomposition, four component decomposition

with rotation of coherency matrix and new general four component decomposition techniques are applied over resized image of region Roorkee of size 400x400.

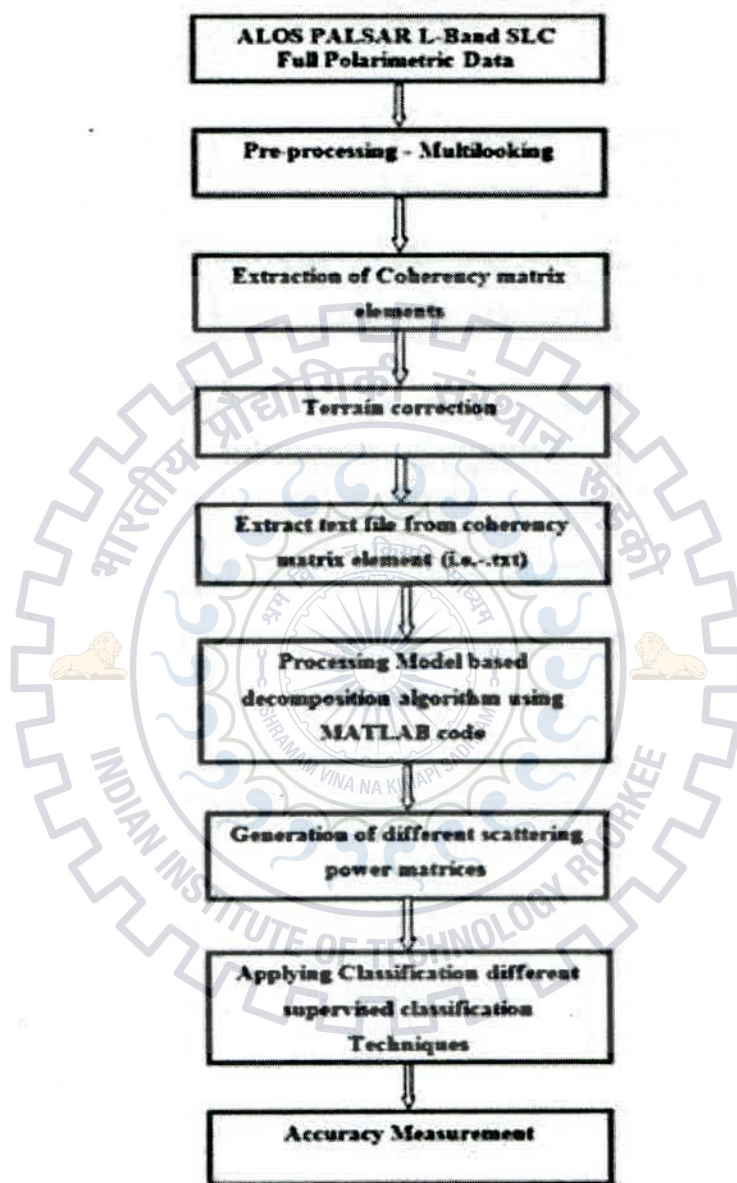


Fig. 4.2: Flow Chart of Methodology

#### ***4.4.1. Data import***

here we are presenting four algorithm based on four different decomposition technique i.e. three component decomposition, four component decomposition, four component decomposition with rotation of coherency matrix and finally The New General decomposition technique.

#### ***4.4.2. Multilooking***

The information you can get fully polarimetric ALOS PALSAR L-Band was in SLC level format (single look complex) 1.1 which means that the data was in the form of the scattering matrix for a single polarization channel (HH, HV, VV and VH) in connection with the complex scattering coefficient. Moreover, the data were not mottled geocoded. This data was in the form of inclined extent, because it is compressed. Therefore, the azimuth resolution, together with the range direction is completely different, 3 m and 21 m respectively. Slant to ground range conversion is conducted away to meet these resolutions. Multiple configurations occurs eyes using 7 looks in azimuth and 1 look in range direction, resulting in an improvement in azimuth resolution from 3 m to about 22m. This resulted in the generation of an image with square pixels due to equalization of azimuth and range resolution. This process is carried out to improve the radiometric measurement accuracy and to reduce speckle, but also reduces the spatial resolution.

#### ***4.4.3. Coherency matrix generation***

In multi-looking method after setting the number of row to 7 and number of column 1 i.e.7 looks in the azimuth direction and 1 look in the range direction, we transformed standard format of data to coherency matrix by using POLSAR PRO software.

#### ***4.4.4. Terrain correction***

Because of the topographical variations of a scene and the inclination of the satellite sensor, the distances can be distorted in the SAR images. Image information is not directly at the Nadir location of the sensor will have certain distortion. Terrain corrections are made to compensate for these distortions so that the geometrical representation of the image will be as close as possible to the real world. For the correction of terrain we used Next ESA SAR Toolbox (NEST) to the output data of multilooking process.

After pre- processing image of size 400x400 was obtained by resizing whole image in order to crop Roorkee region only. This data was converted to ASCII using the ENVI software to be processed through MATLAB. A MATLAB code was written for four different types of decomposition i.e. Freeman decomposition, 4-component decomposition, 4-component decomposition with rotation of coherency matrix and the new general decomposition based on the algorithm[9][10][31][32]. Further, as can be processed through the software ENVI 4.7, and is saved in ".dat file" format from the results of MATLAB code. As a result of these above decompositions three images  $P_d$ ,  $P_v$  and  $P_s$  were obtained corresponding to double bounce scattering, volume scattering and single bounce scattering respectively for freeman decomposition and four images  $P_d$ ,  $P_v$ ,  $P_s$  and  $P_c$  were obtained corresponding to double bounce scattering, volume scattering and single bounce scattering respectively for remaining decomposition techniques. Then, the co-registration of these images was performed by the image to image registration by using the original resized image .

#### 4.4.5. Model based decomposition algorithm

here we are presenting four algorithm based on four different decomposition technique i.e. three component decomposition, four component decomposition, four component decomposition with rotation of coherency matrix and finally The New General decomposition technique.

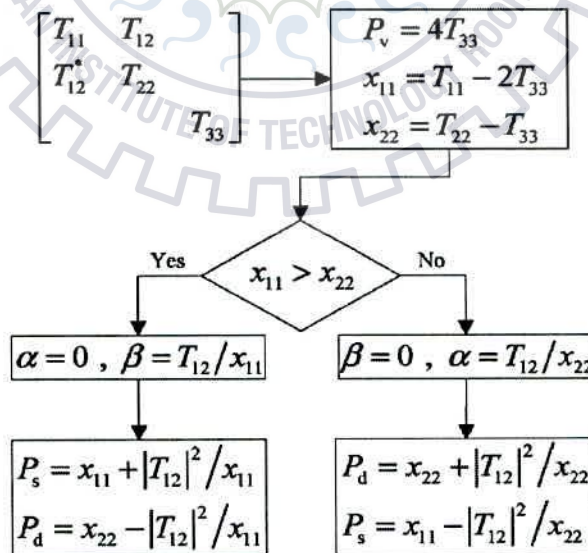


Fig 4.3: Flow Chart of Three Component Decomposition algorithm[9]

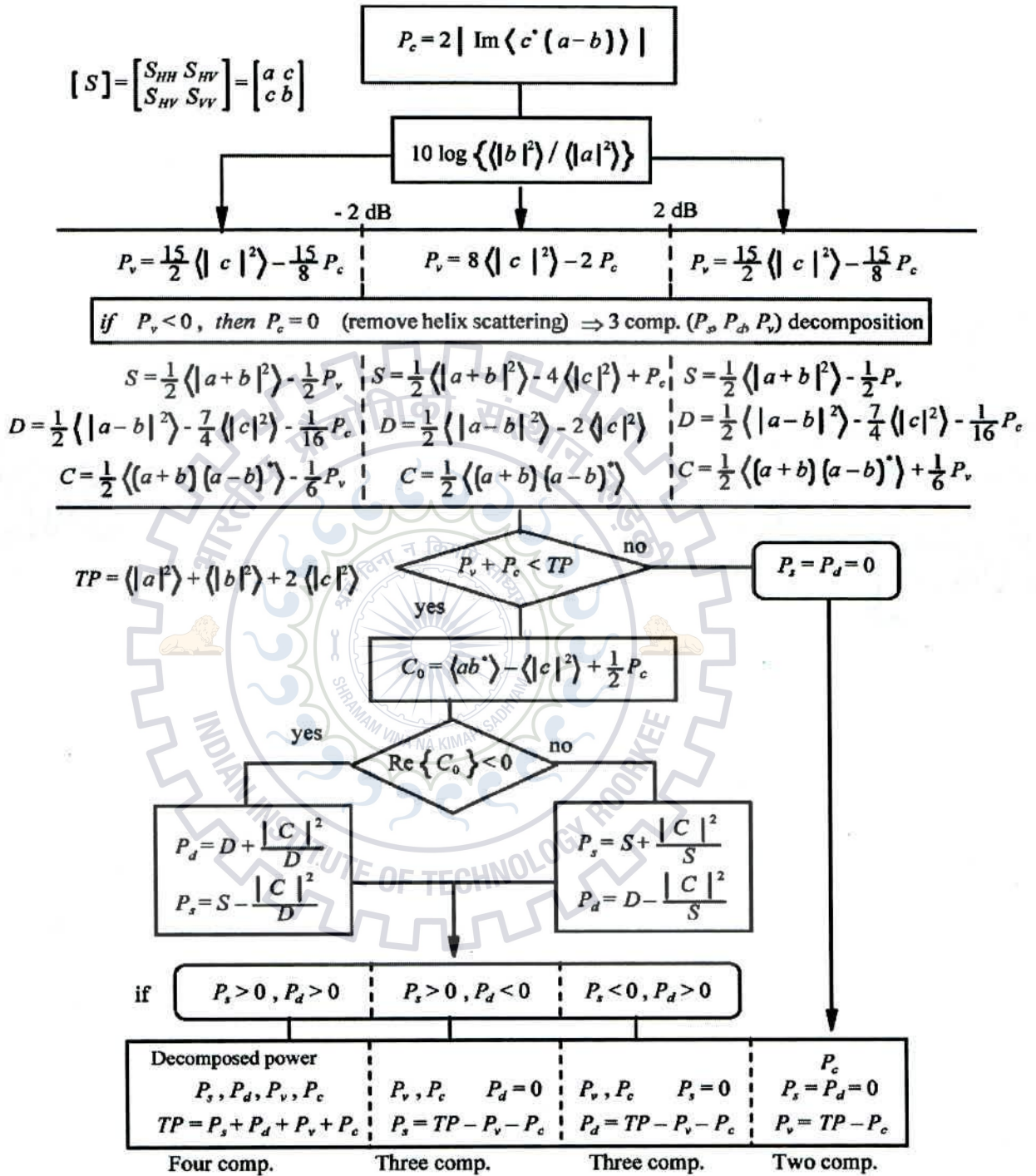


Fig 4.4: Flow Chart of Four Component Decomposition algorithm[10]

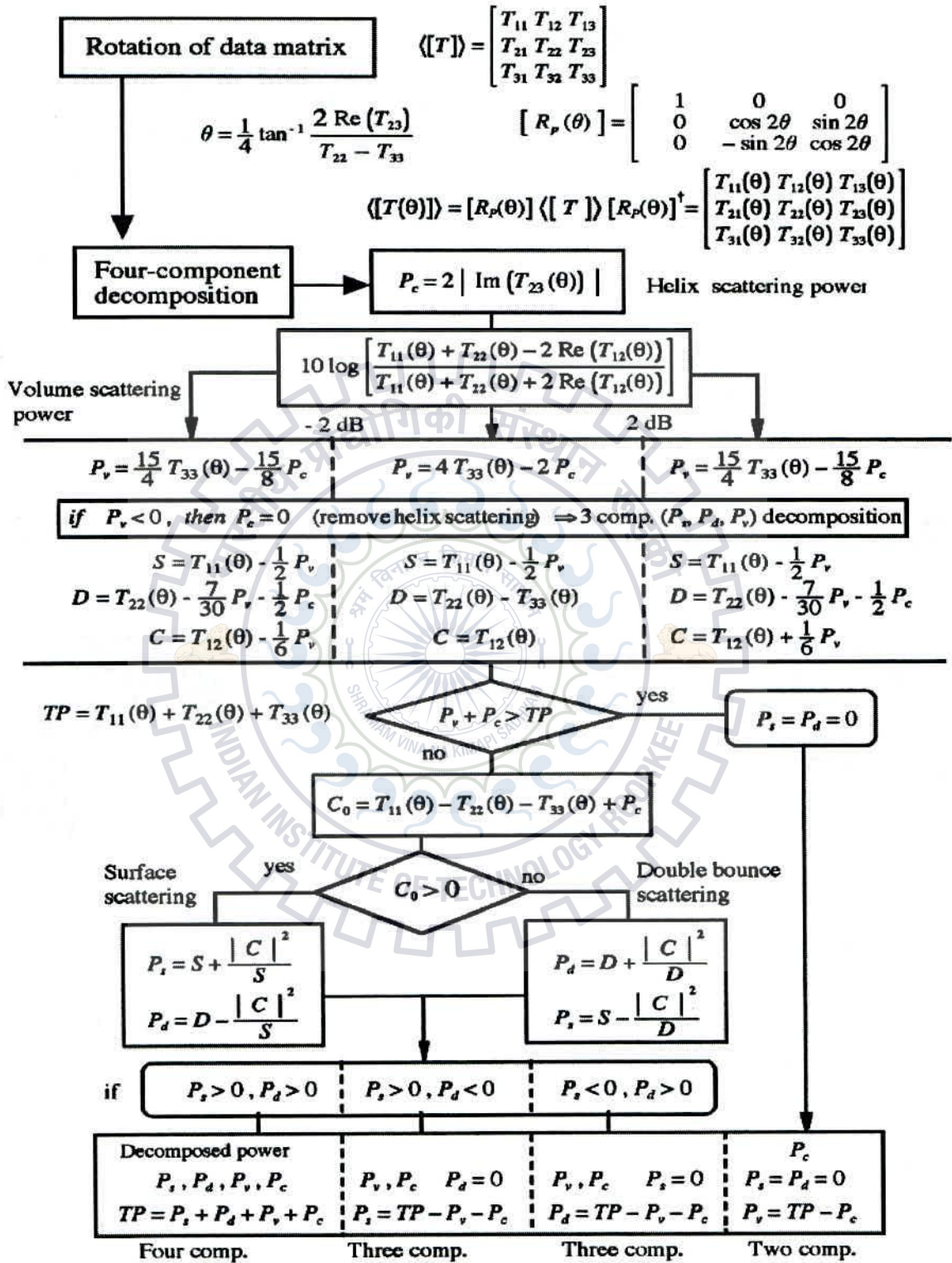


Fig 4.5: Flow Chart of Four Component Decomposition with rotation of coherency matrix.[31]

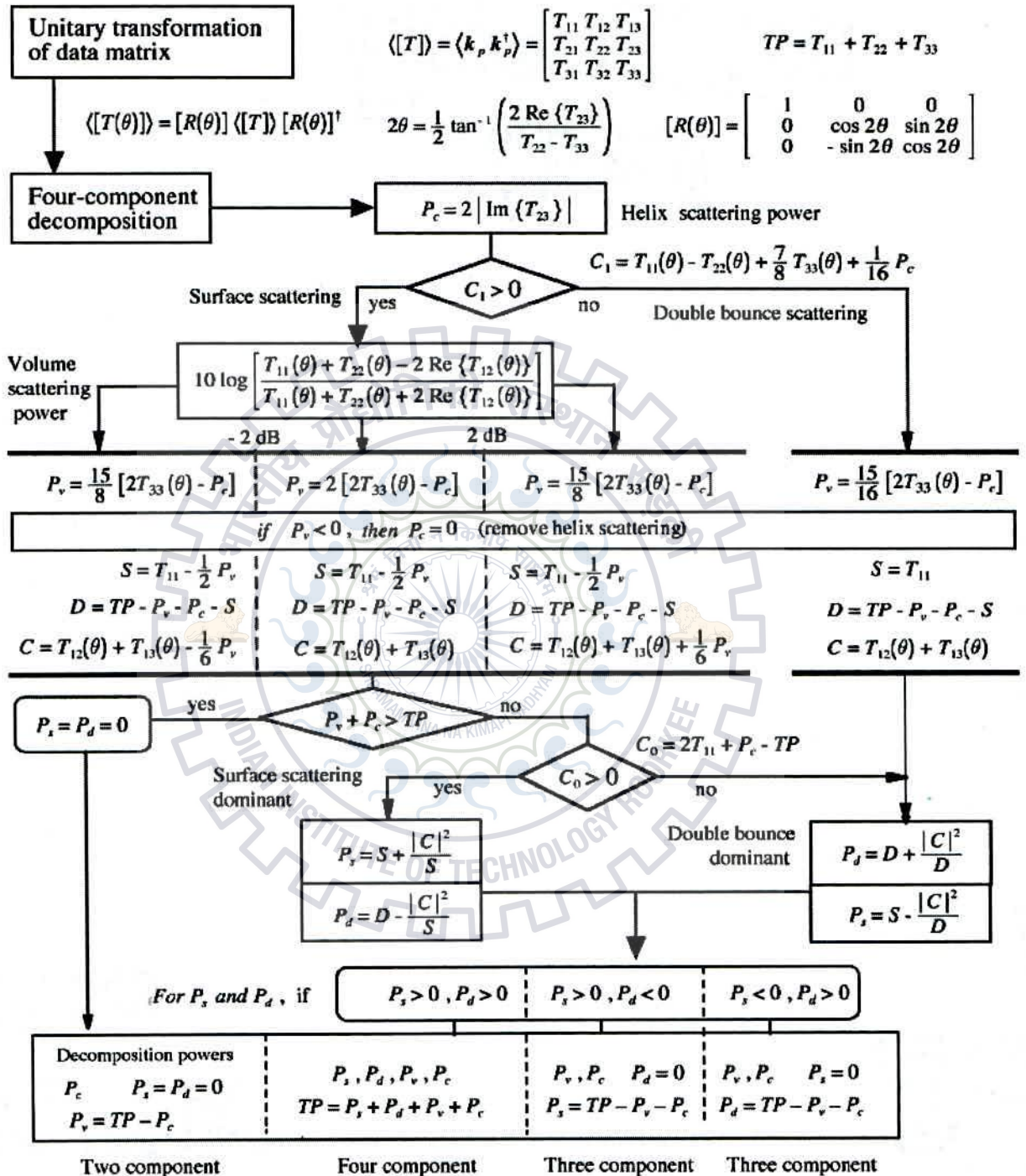


Fig 4.4: Flow Chart of General Four Component Decomposition with unitary transformation of coherency matrix.[32]

#### 4.5. Classification based on Model based Decomposition

The decomposed image obtained as a result of the Four component decomposition, was used for classification herein. Ground truth survey was conducted over the entire area. Around 181 Ground truth points (GCP) were collected for training and 158 for testing the accuracy of classification map shown in table-. Based on ground truth survey four classes were defined: water (includes wetland also), urban, vegetation and bare soil.

Table 4.2: Ground truth survey points for region Roorkee

Sort	Training sample	Test sample
Water	40	38
Urban	63	49
Vegetation	43	39
Bare soil	35	32

We used three supervised classification techniques: minimum distance, parallelepiped and maximum likelihood. We trained these classifiers through 158 ROI's. The result of classification algorithm was calculated using error matrix (or confusion matrix), which compares the classification result with ground truth information and reports overall accuracy, kappa coefficient, producer accuracy and user accuracy. We repeated this procedure for all decomposed images obtained by taking various window sizes in formulation of covariance matrix terms while writing MATLAB code. Then the effect of window size on all the classifications was also seen.



## CHAPTER 5: RESULT AND DISCUSSION

The results obtained from the methods described in the chapters-4 are presented in this chapter. First, all of the results of the main steps of the methodology have been described, together with the observations thereof.

### 5.1. Model based decomposition

The decomposition schemes discussed in this dissertation are applied to ALOS-PALSAR data of Roorkee region. The colour-coded images of Roorkee region are displayed in Fig.6.1. In colour coding scheme double bounce objects is represented by red, volume scattering objects by green and surface scattering objects by blue colour. The close-up view of rectangular areas represent a small area of about 496 pixels for which all parameters i.e.  $P_s$ ,  $P_d$ ,  $P_v$  and  $P_c$  is computed and shown in the figure(5.1.2, 5.2.1, 5.3.1, 5.4.1).

#### 5.1.1. Three Component Decomposition

The scattering contribution i.e. the pixel values from each of the three components was extracted from the three component decomposition results. The total contribution of the three scattering powers i.e.  $P_s$ ,  $P_v$  and  $P_d$ , from the patch was plotted in the form of a pie chart for the three decomposition methods. It can be observed from the figure 5.1.2. that the contribution of the volume scattering power 51.29% and  $P_d$  is 26.51% and  $P_s$  is 22.20% .



Fig:5.1.1: RGB color coding image three component decomposition

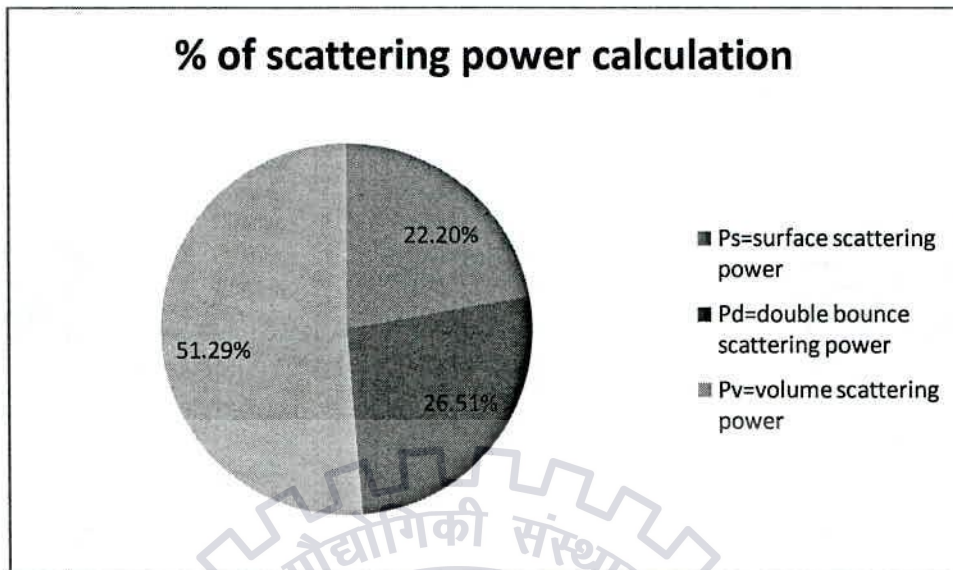


Fig:5.1.2: Percentage share of different scattering power of three component decomposition

**Remark:**

In our study, patch is selected for urban region of Roorkee. Three component decomposition gives more relevant results for natural target i.e. forest region, natural vegetation region. The main reason behind this better result is because of satisfying reflection symmetric condition but in case of urban region, due to non-reflection symmetric condition some negative powers appear in the image analysis[37]. This negative power pixel is attributed by the volume scattering power overestimation after decomposition, i.e., the power of surface and double-bounce may be negative after decomposition. In this decomposition technique, only 5 out of 9 element of coherency matrix is utilized.

**5.1.2.Four component decomposition**

The scattering contribution i.e. the pixel values from each of the four components was extracted from the four component decomposition results. The total contribution of the four scattering powers i.e. Ps, Pv, Pd and Pc from the patch was plotted in the form of a pie chart for the Four decomposition methods. It can be observed from the figure 5.2.2. that the contribution of the scattering power are 45.64%, 29.23%, 22.20% and 3.24% for Pv, Pd, Ps, and Pc respectively. It can also be observed from the above figure that the share of the volume scattering power, which was 51.29% for three component decomposition, get reduced to 45.64% and Pd is increased to 29.23% in case of four component decomposition.

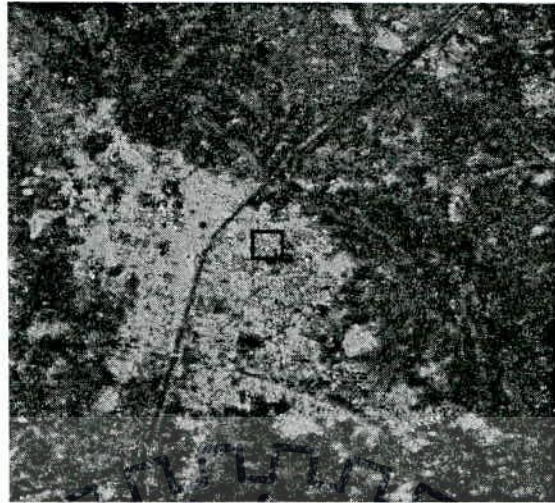


Fig:5.2.1. RGB color coding image Four component decomposition

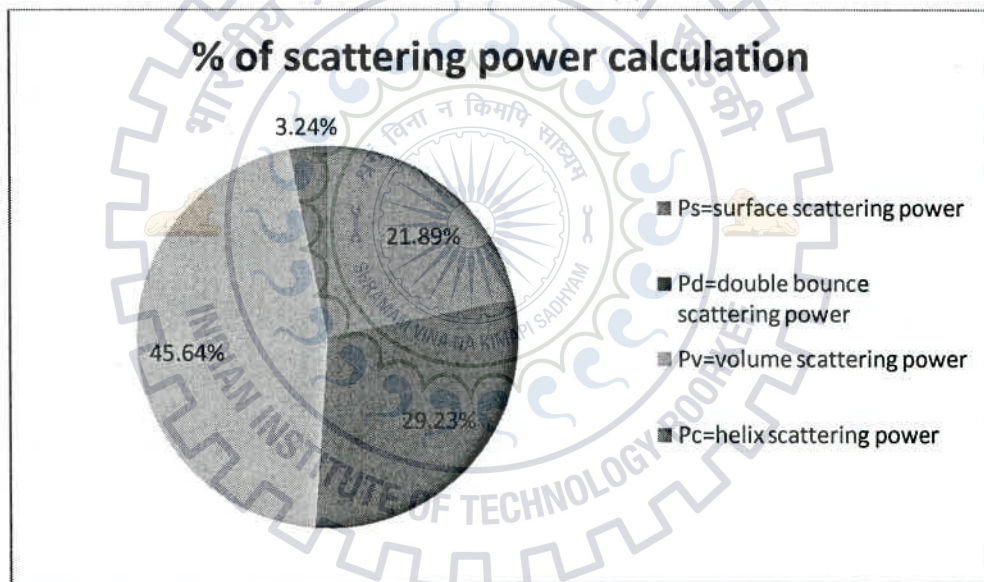


Fig:5.2.2. percentage scattering power of Four component decomposition

**Remark:**

It is concluded that the volume scattering power is decreased and double bounce is increased in fourth component decomposition. A new scattering power called helix power is introduced in four component decomposition which compensates the non-reflection symmetric components and as a result we get decreased value of negative power as compared to former three component decomposition. Mathematically negative power is caused due to excess of cross

polarization which is directly proportional to volume scattering power. In this decomposition scheme, only 6 out of 9 element of coherency matrix is utilized.

### ***5.1.3.Four component decomposition with rotation of coherency matrix***

The scattering contribution i.e. the pixel values from each of the four components was extracted from the four component decomposition results. The total contribution of the four scattering powers i.e.  $P_s$ ,  $P_v$ ,  $P_d$  and  $P_c$  from the patch was plotted in the form of a pie chart for the Four component decomposition with rotation of coherency matrix methods. It can be observed from the below figure that the contribution of the volume scattering power is 41.86% ,  $P_d$  is 32.45% ,  $P_s$  is 22.37% and  $P_c$  is 3.32%. It clear from the above figure(5.1.2,5.2.2) that the contribution of the volume scattering power, which was 51.29% for three component decomposition and in case of four component decomposition it was 45.64%, In four component decomposition with rotation of coherency matrix method, volume scattering power is decreased to 41.86% and  $P_d$  is increased to 32.45%.

#### ***Remark:***

In this decomposition technique we have seen that the volume power is further decreased where as double bounce power is increased. Because in this method T33( which has only cross polarization term) of coherency matrix is minimized. In this decomposition technique, only 6 out of 8 element of coherency matrix is utilized.



Fig:5.3.1. RGB color coding image Four component decomposition with rotation of coherency matrix

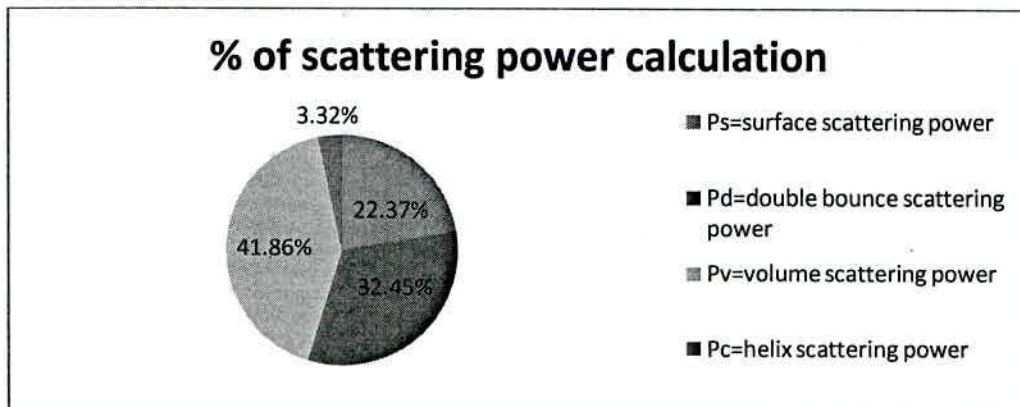


Fig:5.3.2. percentage sharing of scattering power of three component decomposition

#### 5.1.4. The New Four Component Decomposition Method

The scattering contribution i.e. the pixel values from each of the four components was extracted from the four component decomposition results. The total contribution of the four scattering powers i.e. Ps, Pv, Pd and Pc from the patch was plotted in the form of a pie chart for the Four component decomposition with double rotation of coherency matrix methods.

It can be observed from the below figure that the contribution of the volume scattering power 39.63% , Pd is 34.96% ,Ps is 22.23% and Pc is 3.18%. In this decomposition method, it is also found that volume scattering also shows substantial decrement in later techniques as compared to former one. As far as helix and surface scattering is concerned, it doesn't show much variation and double bounce power is substantially increased.

#### Remark

In this decomposition technique we have seen that the volume power is further decreased where as double bounce power is increased. Because in this method T33( which has only cross polarization term )of coherency matrix makes zero by using rotation angle "theta" and again T23 elements of coherency matrix makes zero by using rotation of angle  $\psi$  In this decomposition technique, so that 7 out of 7 element of coherency matrix is utilized i.e. full utilization of coherency matrix and hence it gives better result as compare to former mentioned method.



Fig 5.4.1. RGB color coding image of The New General Component Decomposition

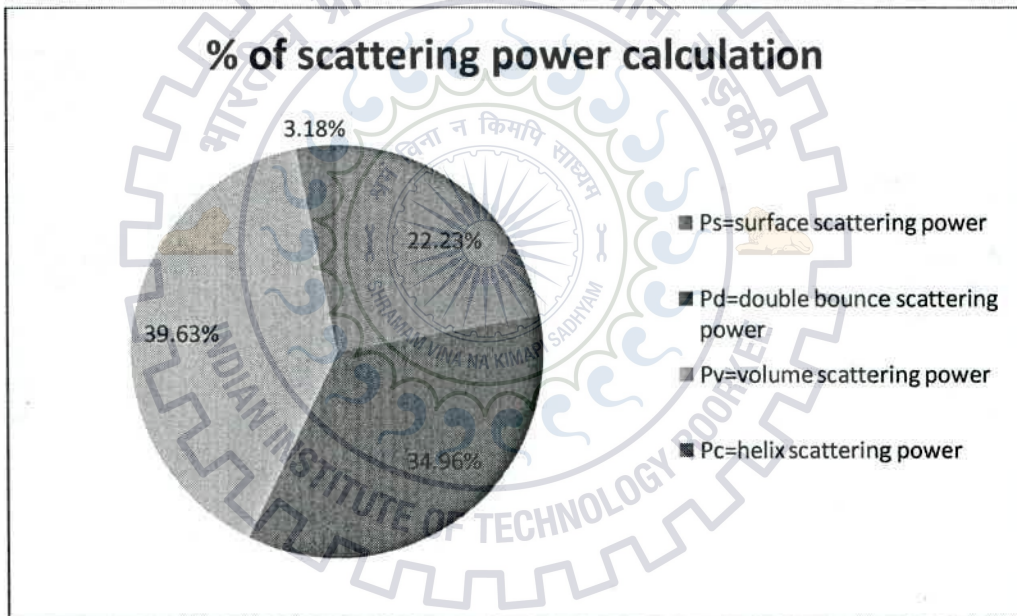


Fig:5.4.2. percentage scattering power of the new General Decomposition component decomposition

## 5.2. SUPERVISED CLASSIFICATION

### 5.2.1. Supervised classification based on 4-component decomposition method.

The classification tests based on 4-component decomposition is performed by supervised classification i.e. Minimum distance, Maximum likelihood and Parallelepiped classifiers. The experiment is performed using all four scattering power components i.e. Ps, Pd, Pv and Pc. The producer and user accuracy estimates relative changes as compared to supervised classification for original 4-component decomposition are shown in Table 5.2.2. The overall classification accuracy of maximum likelihood is obtained as 72.1519% and kappa coefficient was 0.6316. Parallelepiped classifier with overall accuracy of 50.6329% and kappa coefficient of 0.3548. The overall classification accuracy for minimum distance classifier lies in between that of maximum likelihood and parallelepiped classifier which is 61.39% with kappa coefficient of 0.4814. Parallelepiped classifier fails to identify 'water' as well as 'urban' classes. but Parallelepiped classifier give good accuracy in identifying baresoil and forest classes. Minimum distance classifier identifies water very nicely but it fails to identify bare soil. Finally, maximum likelihood classifier gives moderate result to identify the all classes. So it gives good accuracy.

Table 5.2.1: Pixel assignment of various classes shown by confusion matrix relative to parallelepiped classification

class	Bare soil test	Forest test	Urban test	Water test
Bare soil	100	0	0.00	36.08
forest	0	100	81.63	57.59
Urban	0	0	18.37	6.33
water	0	0	0	0

Table 5.2.2: User accuracy and producer accuracy (in percent) estimates relative to parallelepiped classification

Classes	P.A.(%)	U.A.(%)
Bare soil	100	56.14
Forest	100	42.86
Urban	18.37	90.00
Water	0	0

Table 5.2.3: User accuracy and producer accuracy (in percent) estimates relative to minimum distance classifier

class	Bare soil test	Forest test	Urban test	Water test
Bare soil	6.25	12.82	4.08	13.16
forest	0	71.79	24.49	2.63
Urban	0	7.69	71.43	0
water	93.75	7.69	0	84.21

Table 5.2.4: Pixel assignment of various classes shown by confusion matrix relative to minimum distance classification

Classes	P.A.(%)	U.A.(%)
Bare soil	6.25	88.29
Forest	71.79	64.86
Urban	71.43	94.87
Water	84.21	62.07

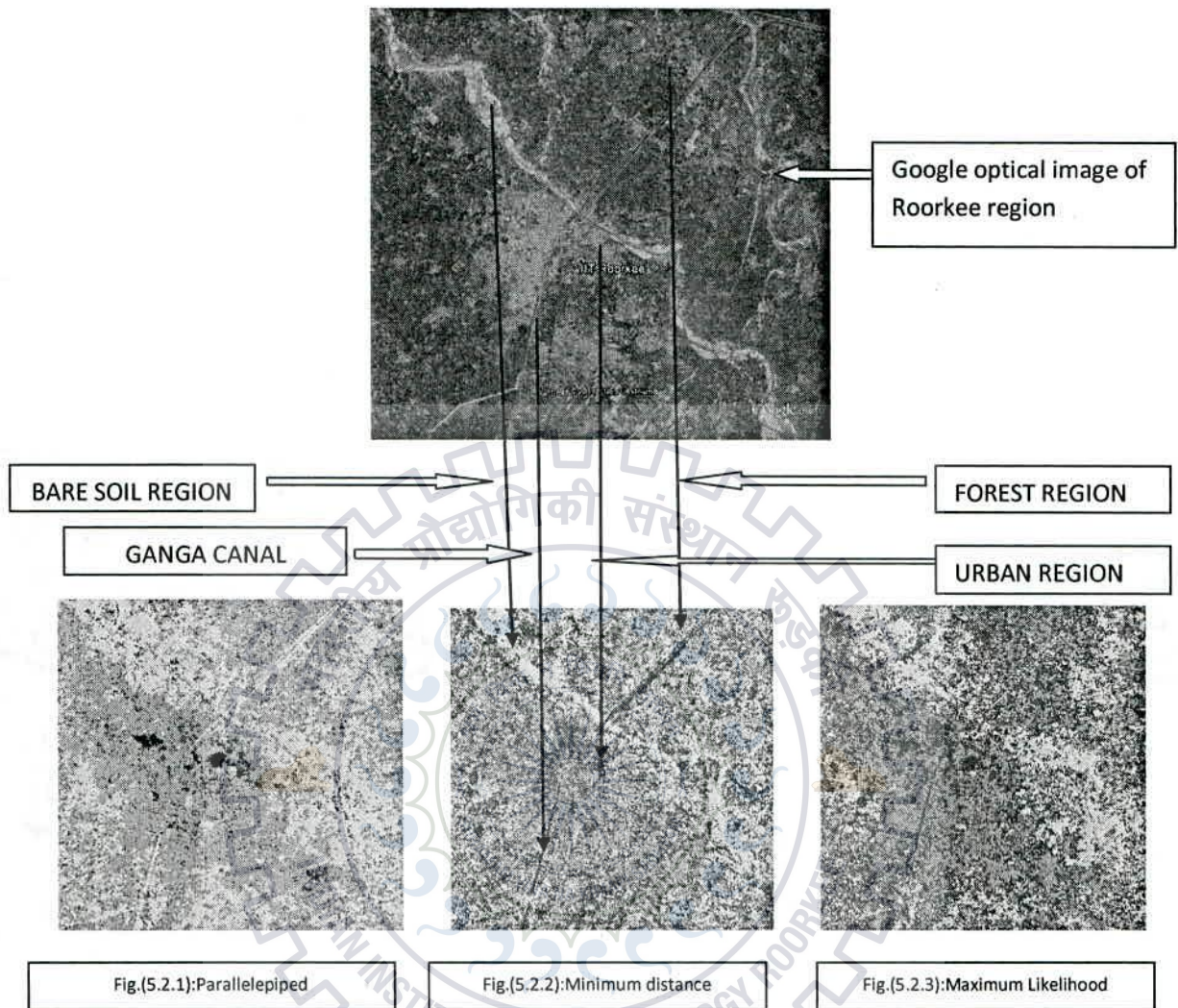


Table 5.2.5: User accuracy and producer accuracy (in percent) estimates relative to minimum distance classifier

class	Bare soil test	Forest test	Urban test	Water test
Bare soil	100	0	0.00	47.37
forest	0	89.74	40.82	5.26
Urban	0	2.56	59.18	0
water	3.13	7.69	0	47.37

Table 5.2.6: Pixel assignment of various classes shown by confusion matrix relative to minimum distance classification

Classes	P.A. (%)	U.A. (%)
Bare soil	100	64.00
Forest	89.74	61.40
Urban	59.18	96.67
Water	47.37	85.71



### 5.2.2. Supervised classification based on 4-component decomposition with rotation of coherency matrix.

The 4-component decomposition with rotation of coherency matrix has been chosen as the basis for the supervised classification. Based on 4-component with rotation of coherency matrix, for classification tests, producer accuracy estimates have been shown in Table (5.3.2, 5.3.4, 5.3.6). The experiment is accomplished with the help of all four scattering power components i.e.  $P_s$ ,  $P_d$ ,  $P_v$  and  $P_c$ . The classification accuracy is maximum for maximum likelihood classifier with overall accuracy of 74.6835% and kappa coefficient of 0.6638, parallelepiped classifier with overall accuracy of 50.36% and kappa coefficient of 0.3554. The overall classification accuracy

for minimum distance classifier lies in between that of maximum distance and parallelepiped classifier which is 58.8608% with kappa coefficient of 0.4504. Some limits are shown by parallelepiped classifier in classifying classes "water" and "urban". This classification technique completely fails in recognizing training pixels related to class "water" and classifies class "urban". Because the class "water" is misclassified. Maximum likelihood classifier identifies all the training pixels more accurately than others and classifies all land cover types with satisfactory performance indices, since each class has quite good producer accuracy. Minimum distance classifier also shows almost the same results. It classifies class "water" more accurately than maximum likelihood classifier.

Table 5.3.1: User accuracy and producer accuracy (in percent) estimates relative to parallelepiped classification

class	Bare soil test	Forest test	Urban test	Water test
Bare soil	100	0	0.00	68.42
forest	0	100	81.63	31.58
Urban	0	0	18.37	5.70
water	100	0	0	0

Table 5.3.2: Pixel assignment of various classes shown by confusion matrix relative to parallelepiped classification

Classes	P.A.(%)	U.A.(%)
Bare soil	100	55.17
Forest	100	42.86
Urban	18.37	100
Water	0	0

Table 5.3.3: User accuracy and producer accuracy (in percent) estimates relative to minimum distance classification

class	Bare soil test	Forest test	Urban test	Water test
Bare soil	3.13	12.82	0.00	5.26
forest	0	84.62	51.02	2.63
Urban	0	0	48.98	0
water	96.88	2.56	0	92.11

Table 5.3.4: Pixel assignment of various classes shown by confusion matrix relative to minimum distance classification



Classes	P.A. (%)	U.A. (%)
Bare soil	3.13	12.50
Forest 	84.62	55.93 
Urban	48.98	100
Water	92.11	52.24

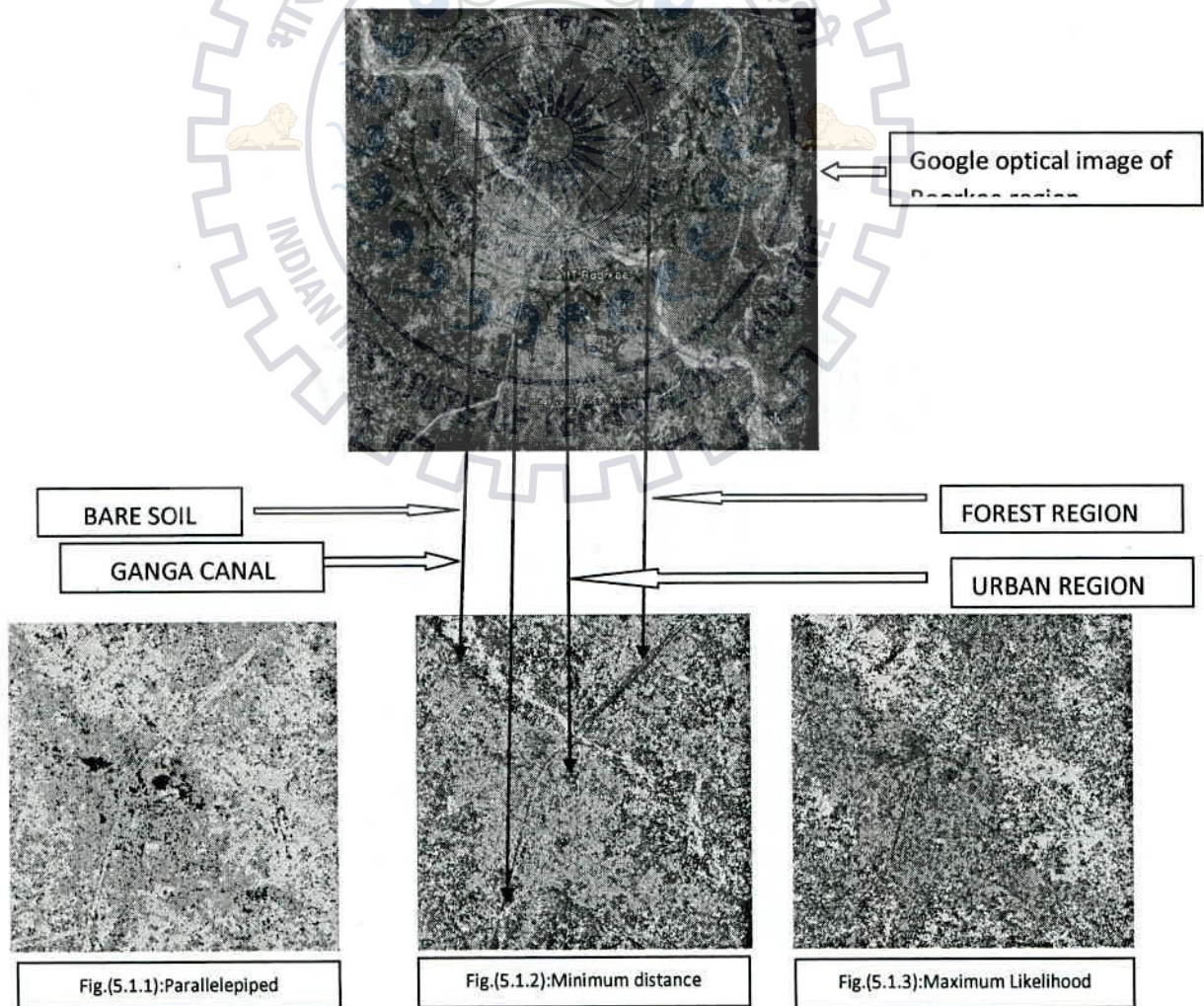
Table 5.3.5: User accuracy and producer accuracy (in percent) estimates relative to minimum distance classification

class	Bare soil test	Forest test	Urban test	Water test
Bare soil	93.75	0	0.00	42.11
forest	0	87.18	30.61	5.26
Urban	0	2.56	69.39	0
water	6.25	10.24	0	52.63



Table 5.3.6: Pixel assignment of various classes shown by confusion matrix relative to minimum distance classification

Classes	P.A.(%)	U.A.(%)
Bare soil	93.75	65.22
Forest	87.18	66.67
Urban	69.39	97.14
Water	52.63	74.92



**5.2.3. Supervised classification based on new general 4-CSPD with unitary transformation (G4U)**

The classifications tests are carried out through these supervised classification techniques i.e. Minimum distance, Maximum likelihood and Parallelepiped which are based on New genera 4-component decomposition with unitary transformation method. All four scattering power components i.e. Ps, Pd, Pv and Pc. are used to demonstrate the results. The producer and user accuracy estimates relative to supervised classification for original 4-component decomposition are shown in Table(5.4.2, 5.4.4, 5.4.6). The overall classification accuracy of maximum likelihood is obtained as 70.8861% and kappa coefficient was 0.6140. In case of Parallelepiped classifier, the overall accuracy is 48.1013% and kappa coefficient is 0.3222. The overall classification accuracy for minimum distance classifier lies in between that of maximum likelihood and parallelepiped classifier which is 60.1266% with kappa coefficient of 0.4642.

Table 5.4.1: User accuracy and producer accuracy (in percent) estimates relative to parallelepiped classification

class	Bare soil test	Forest test	Urban test	Water test
Bare soil	96.88	5.13	0.00	60.53
forest	3.13	94.87	83.67	39.47
Urban	0	0	16.33	0
water	0	0	0	0

Table 5.4.2: Pixel assignment of various classes shown by confusion matrix relative to parallelepiped classification

Classes	P.A.(%)	U.A.(%)
Bare soil	96.88	55.36
Forest	94.87	39.36
Urban	16.33	100
Water	0.00	0.00

Table 5.4.3: User accuracy and producer accuracy (in percent) estimates relative to minimum distance classification.

class	Bare soil test	Forest test	Urban test	Water test
Bare soil	9.38	5.13	0	28.57
forest	0	84.62	28.57	7.89
Urban	0	10.26	71.43	0
water	90.63	0	0	63.16

Table 5.4.4: Pixel assignment of various classes shown by confusion matrix relative to minimum distance classification

Classes	P.A.(%)	U.A.(%)
Bare soil	9.38	18.75
Forest	84.62	66.00
Urban	71.43	89.74
Water	63.16	45.28

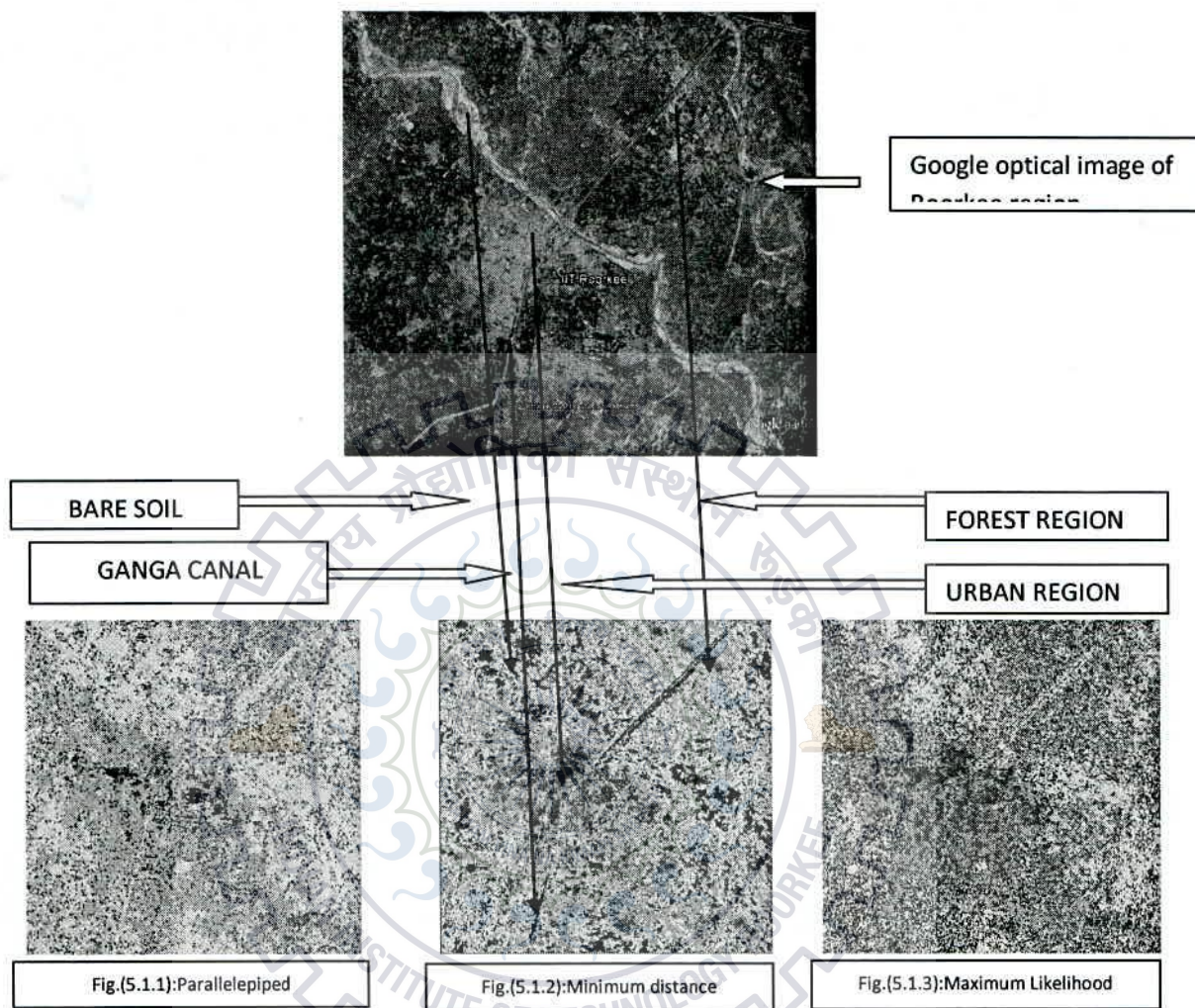


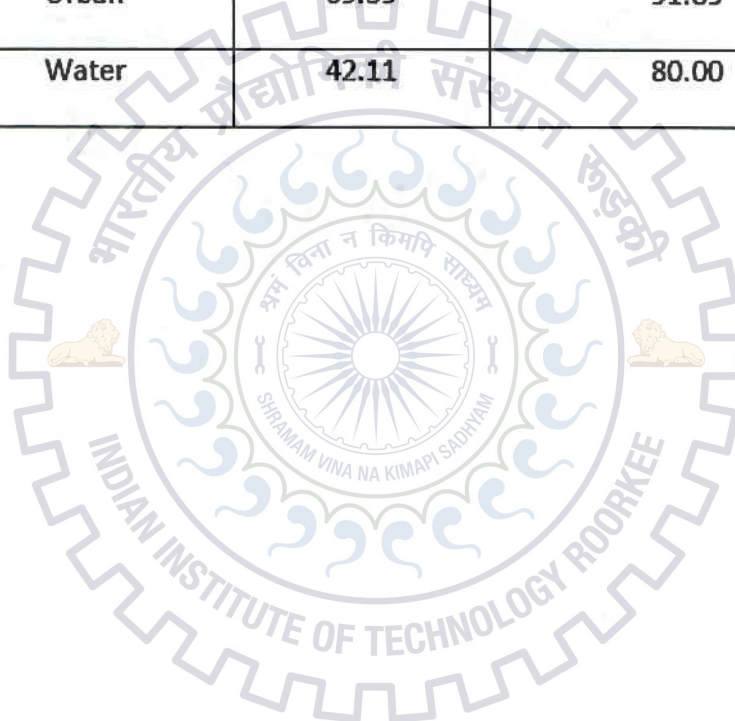
Table 5.4.5: User accuracy and producer accuracy (in percent) estimates relative to minimum distance classification

class	Bare soil test	Forest test	Urban test	Water test
Bare soil	96.88	5.13	0.00	55.26
forest	0	79.49	30.61	2.63
Urban	0	7.69	69.39	0
water	3.13	7.69	0	42.11



Table 5.4.6: Pixel assignment of various classes shown by confusion matrix relative to minimum distance classification

Classes	P.A.(%)	U.A.(%)
Bare soil	96.88	57.41
Forest	79.49	65.96
Urban	69.39	91.89
Water	42.11	80.00



## CHAPTER 6: CONCLUSION AND FUTURE SCOPE

A model based different decomposition techniques were studied and critically evaluated. For evaluation purpose, pixel level percentage of different scattering phenomena has been computed as well as supervised classifier is used to see the effect of different decomposition techniques on land cover classification. This classification scheme is applied to fully polarimetric ALOS PALSAR L-1.1 data. Four classes are identified: water, urban, vegetation, and bare soil. Percentage of scattering power is analyzed for different decomposition techniques for a single specified region (black squared patch). We have performed land cover classification, based on SAR observables obtained 4-component decomposition, 4-component decomposition with rotation of coherency matrix and General 4-CSPD with Unitary Transformation. The Maximum likelihood classifier recognizes all land cover types more accurately from training pixel than parallelepiped, minimum distance. The conclusion after applying supervised classification techniques using three decomposition methods (4-component decomposition, 4-component decomposition with rotation of coherency matrix and General 4-CSPD with Unitary Transformation) is that 4-component decomposition with rotation of coherency matrix gives the better results as compared to others.

### *Future scope*

Having additional land cover/use classes could be beneficial for further research. Research oriented towards incorporating a higher number of complex land cover/use classes would be useful for uncovering some of the additional functionality of the quad polarization radar datasets. Secondly, evaluating the classification accuracies for larger texture window sizes would also be important.

Third is the improvement of classification by applying various kinds of filtering techniques for speckle reduction and collection of more amounts of ground truth survey points may be an added research area to work upon. By doing so, the number of points along with number of training samples can be increased which may lead to much more accurate assessments. Thus, in all we can say that improvement of classification accuracy can be achieved by increasing the number of training and testing ground truth sample points.

## REFERENCES

- [1] P. Mishra and d. Singh, "land cover classification of palsar images by knowledge based decision tree classifier and supervised classifiers based on sar observables", progress in Electromagnetics research , vol. 30, 47-70, 2011.
- [2] Evanny Obregon, Ki Won Sung and Jens Zander, "Secondary Access to the Radar Spectrum Bands: Regulatory and Business Implications", European regional conference of the international telecommunications society, florence,italy, 2013.
- [3] Triloki Pant, D. Singh and Tanuja Srivastava "Advanced Fractal Approach for Unsupervised Classification of SAR Images", Advances in Space Research, 45, 1338- 1349, 2010.
- [4] Parul Patel , H. S. Srivastava, and R. R. Navalgund, "Use of synthetic aperture radar polarimetry to characterize wetland targets of Keoladeo National Park, Bharatpur, India," Research article ,Current Science, vol. 97, no. 4,pp. 529-537, 2009.
- [5] Cloude, S. R. and E. Pottier, A review of target decomposition theorems in radar polarimetry," IEEE Transactions on Geoscience and Remote Sensing, Vol. 34, No. 2, 498-518, 1996.
- [6] Enderle, D. I. M. and R. C. Weih Jr., Integrating supervised and unsupervised classification methods to develop a more accurate land cover classification," Journal of the Arkansas Academy of Science, Vol. 59, 65-73, 2005.
- [7] Hui, Y., et al., Extracting wetland using decision tree classification," Proceedings of the 8th WSEAS International Conference on Applied Computer and Applied Computational Science", 240-245, 2004.
- [8] S. R. Cloude and E. Pottier, "A review of target decomposition theorems in radar polarimetry," IEEE Trans. Geosci. Remote Sensing, vol. 34, no. 2, pp. 498-518, Mar. 1996.
- [9] Freeman and S. L. Durden, "A three-component scattering model for polarimetric SAR data,"IEEE Transactions on Geoscience and Remote Sensing, vol. 36, no. 3, pp. 963-973, May 1998.

- [10] Yoshio Yamaguchi, Toshifumi Moriyama, Motoi Ishido, and Hiroyoshi Yamada, "Four-component scattering model for polarimetric SAR image decomposition", IEEE Transactions on Geoscience And Remote Sensing, vol. 43, no. 8, pp. 1699- 1706, 2005.
- [11] <http://en.wikipedia.org/wiki/Polarizer>
- [12] H. Zebker, and VanZyl , "Imaging Radar Polarimetry: A Review", Proceedings of the IEEE, vol. 79, no. 11, 2001.
- [13] Pottier et al., 'Bistatic radar polarimetry theory,' chapter 14 in James D. Taylor (ed.), Ultra wideband radar technology, CRC press, e-book ISBN-978-1-4200-3729-6, 2001.
- [14] J. Fransis Reintjes et al., Principles of Radar, third edition, McGraw-Hill book company, Inc., New York, 1952.
- [15] J.-S. Lee and E. Pottier, Polarimetric Radar Imaging: From Basics to Applications, 1st ed. CRC Press, 2009.
- [16] Canada Centre for Remote Sensing, "Advanced Radar Polarimetry Tutorial," Available: [http://www.ccrs.nrcan.gc.ca/resource/tutor/polarim/pdf/polarim\\_e.pdf](http://www.ccrs.nrcan.gc.ca/resource/tutor/polarim/pdf/polarim_e.pdf). [Accessed: 25-may-2014].
- [17] J.-S. Lee and E. Pottier, Polarimetric Radar Imaging: From Basics to Applications, 1st ed. CRC Press, 2009.
- [18] J. A. Richards, Remote Sensing with Imaging Radar. Springer, 2009.
- [19] D. Massonnet and J.-C. Souyris, Synthetic Aperture Radar Imaging. EFPL Press, 2008.
- [20] Canada Centre for Remote Sensing, "Educational Resources for Radar Remote Sensing," [www.ccrs.nrcan.gc.ca](http://www.ccrs.nrcan.gc.ca), 18-Oct-2011. [Online]. [Accessed: 14-Feb-2012].
- [21] Principles of remote sensing, Paul J. Curran, Longman, London and New York, 1985.
- [22] S. R. Cloude and E. Pottier, "A review of target decomposition theorems in radar polarimetry," IEEE Trans. Geosci. Remote Sensing, vol. 34, no. 2, pp. 498-518, Mar. 1996.
- [23] A. Freeman and S. L. Durden, "Three-component scattering model to describe polarimetric SAR data," Proceedings of SPIE, vol. 1748, no. 1, pp. 213-224, Feb. 1993.
- [24] H. Kimura, "Radar Polarization Orientation Shifts in Built-Up Areas," IEEE Geoscience and Remote Sensing Letters, vol. 5, no. 2, pp. 217-221, Apr. 2008.
- [25] H. Kimura, K. P. Papathanassiou, and I. Hajnsek, "Polarization orientation effects in urban areas on SAR data," in Geoscience and Remote Sensing Symposium, 2005. IGARSS '05. Proceedings. 2005 IEEE International, 2005, vol. 7, pp. 4863- 4867

- [26] K. Iribe and M. Sato, "Analysis of polarization orientation angle shifts by artificial structures," *IEEE TRANSACTIONS ON GEOSCIENCE AND REMOTE SENSING*, vol. 45, no. 11, pp. 3417-3425, Nov. 2007.
- [27] E. Krogager, W. Boerner, and S. Madsen, "Feature-motivated Sinclair matrix (sphere/diplane/helix) decomposition and its application to target sorting for land feature classification," *WIDEBAND INTERFEROMETRIC SENSING AND IMAGING POLARIMETRY*, vol. 3120, pp. 144-154, 1997.
- [28] Lamei Zhang, Bin Zou, Hongjun Cai, and Ye Zhang, "Multiple-Component Scattering Model for Polarimetric SAR Image Decomposition," *IEEE Geoscience and Remote Sensing Letters*, vol. 5, no. 4, pp.603-607, Oct. 2008.
- [29] European Space Agency, "Single Multi Polarization SAR data," [www.envisat.esa.int](http://www.envisat.esa.int), 18-Sep-2011.
- [30] J.-S. Lee and E. Pottier, *Polarimetric Radar Imaging: From Basics to Applications*, 1st ed. CRC Press, 2009.
- [31] Yoshio Yamaguchi, Akinobu Sato, Ryoichi Sato, Hiroyoshi Yamada, Wolfgang -m. Boerner "four-component scattering power decomposition With rotation of coherency matrix" vol.3, no. 4, pp. 555-559, oct. 2011.
- [32] Gulab Singh, Yoshio Yamaguchi, and Sang-Eun Park, "General Four-Component Scattering Power Decomposition With Unitary Transformation of Coherency Matrix" *IEEE Transactions On Geoscience And Remote Sensing*, Vol. 51, No. 5, May 2013.
- [33] J.S. Lee, M.R. Grunes, Eric Pottier, and L. Ferro-Famil "Unsupervised terrain classification preserving polarimetric scattering characteristics," vol. 42, no. 4, 2004.
- [34] J.S. Lee, M.R. Grunes, T.L. Ainsworth, L. Du, D.L. Schuler and S.R. Cloude "Unsupervised classification of polarimetric SAR images by applying target decomposition and complex Wishart distribution," *IEEE Trans. on Geoscience and Remote Sensing*, vol.37, no.5, pp. 2249-2258, 1999.
- [35] Brandt Tso, Paul Mather, *Classification Methods for Remotely Sensed Data*, 2nd ed. CRC Press, Taylor & Francis Group, LLC, 2009.
- [36] J.A. Richards, *Remote Sensing Digital Image Analysis*, Springer-Verlag, Berlin, 1999.